Kalita et al. Earth, Planets and Space (2015) 67:186
DOI 10.1186/s40623-015-0355-3

Earth, Planets and Space
a SpringerOpen Journal

FULL PAPER Open Access

NmF2 and hmF2 measurements at 95° E and 127° E around the EIA northern crest during 2010–2014

Bitap Raj Kalita[1*], Pradip Kumar Bhuyan[1] and Akimasa Yoshikawa[2]

Abstract

The characteristics of the F2 layer parameters NmF2 and hmF2 over Dibrugarh (27.5° N, 95° E, 17° N geomagnetic, 43° dip) measured by a Canadian Advanced Digital Ionosonde (CADI) for the period of August 2010 to July 2014 are reported for the first time from this low mid-latitude station lying within the daytime peak of the longitudinal wave number 4 structure of equatorial anomaly (EIA) around the northern edge of anomaly crest. Equinoctial asymmetry is clearly observed at all solar activity levels whereas the midday winter anomaly is observed only during high solar activity years and disappears during the temporary dip in solar activity in 2013 but forenoon winter anomaly can be observed even at moderate solar activity. The NmF2/hmF2 variations over Dibrugarh are compared with that of Okinawa (26.5° N, 127° E, 17° N geomagnetic), and the eastward propagation speed of the wave number 4 longitudinal structure from 95° E to 127° E is estimated. The speed is found to be close to the theoretical speed of the wave number 4 (WN4) structure. The correlation of daily NmF2 over Dibrugarh and Okinawa with solar activity exhibits diurnal and seasonal variations. The highest correlation in daytime is observed during the forenoon hours in equinox. The correlation of daily NmF2 (linear or non-linear) with solar activity exhibits diurnal variation. A tendency for amplification with solar activity is observed in the forenoon and late evening period of March equinox and the postsunset period of December solstice. NmF2 saturation effect is observed only in the midday period of equinox. Non-linear variation of neutral composition at higher altitudes and variation of recombination rates with solar activity via temperature dependence may be related to the non-linear trend. The noon time maximum NmF2 over Dibrugarh exhibits better correlation with equatorial electrojet (EEJ) than with solar activity and, therefore, new low-latitude NmF2 index is proposed taking both solar activity and EEJ strength into account.

Keywords: WN4 structure, NmF2, hmF2, Solar activity, Saturation, Amplification, EEJ

Introduction

The earth's ionosphere is formed due to photoionization of neutral atmosphere by solar radiation and exhibits latitudinal, longitudinal, altitudinal as well as diurnal and seasonal variations. The behavior of the ionosphere depends on the structure of geomagnetic field and geomagnetic activity in addition to the solar flux (Field and Rishbeth 1997; Buonsanto 1999; Danilov and Lastovicka 2001; Simi et al. 2013, etc). The distribution of ionization in low-latitude ionosphere particularly the F2 layer is affected by the equatorial ionization anomaly (Appleton 1946). The characteristics of the ionosphere also changes with longitude (Bailey 1948; Thomas 1968), and there are important differences in Asian, African, and American zones (Rao 1963a). Walker (1981) reported significant longitudinal variation using only ionosonde data. Deminova (1993, 1995) first reported a wavelike longitudinal structure of the critical frequency of the F2 layer both along the equator and the anomaly crest using data from the Intercosmos II satellite. Later, Sagawa et al. (2005) reported wavelike structure in the development of EIA during March–June of 2002, at nighttime by analyzing the OI 135.6-nm nightglow from far ultraviolet imager (FUV) on board the IMAGE satellites and thereby suggested a

* Correspondence: bitapkalita@dibru.ac.in
[1]Center for Atmospheric Studies, Dibrugarh University, Dibrugarh 786004, Assam, India
Full list of author information is available at the end of the article

longitudinal structure with wave number 4 (WN4) or 90° periodicity. England et al. (2006) have shown from CHAMP, Ørsted, and SAC-C satellite observation the existence of longitudinal structure in noon time equatorial electrojet (EEJ) similar to nighttime EIA structure. Immel et al. (2006) and Lin et al. (2007a) have postulated that atmospheric tides are the source of the WN4 phenomenon. Using TOPEX Total Electron Content (TEC) data, Scherliess et al. (2008) have found that the WN4 structure is created in low-latitude TEC in equinox and June solstice with enhancement along the 100° E, 190° E, 270° E, and 10° E. Lühr et al. (2007) have reported a four-peaked longitudinal structure in electron density and zonal wind measured by the CHAMP satellite at 400 km. Kil et al. (2007) and Oh et al. (2008) reported the existence of a structure of four peaks of enhanced plasma density along the equatorial anomaly even at the topside of F region near 10° E, 100° E, 200° E, and 280°E and showed its relation to the vertical E × B drift. Liu and Watanabe (2008) from CHAMP satellite data have observed significant seasonal variation of the longitudinal plasma density structure at fixed solar activity levels. It has also been shown (Sagawa et al. 2005; Immel et al. 2006; Oh et al. 2008) that along these four high-density regions, the anomaly crest moves poleward to higher magnetic latitude. Using FORMOSAT-3/COSMIC (F3/C) satellite constellation, Lin et al. (2007b) have shown that the four-peaked EIA longitudinal structure evolve with local time and tend to move eastward with velocity of several tens of meters per second. The eastward shifting of the location of the daytime peak of the WN4 structure by around 20° was also reported by Liu and Watanabe (2008), Scherliess et al. (2008) and Fang et al. (2009). In particular, the daytime peak along 90–100° E moves to around 120° E by nighttime. The longitudinal WN4 structure also exhibits some altitudinal difference (Kil et al. 2007) particularly at nighttime. The longitudinal structure of plasma density has been detected by different techniques and in different altitude. The optical observations (Sagawa et al. 2005; Henderson et al. 2005; Immel et al. 2006) provide information of the density near the F region. The measurements by ROCSAT-1 (Kil et al. 2007; Kil et al. 2008; Oh et al. 2008; Fang et al. 2009) basically give a picture of the topside density structure. The TEC measurements (Scherliess et al. 2008) and the radio occultation measurements (Lin et al. 2007a, 2007b) are altitude independent. Recently, Bhuyan and Hazarika (2012) and Watthanasangmechai et al. (2015) have reported the characteristics of TEC along 95–100° E which is within the most prominent peak of the WN4 structure at 100° E during the ascending phase of solar cycle 2009–2012, but no bottom side (ionosonde) measurements have been reported from this region yet. Satellite- and ground-based methods are complementary in many respects (Booker and Smith 1970) and ground-based ionosondes provide valuable information of vertical ionospheric structure. Lin et al. (2007a) have shown that the wave number 4 longitudinal structure mainly exists in the F region of the ionosphere or above 250–300 km, and therefore, measurements of the F layer by the ionosonde in these sectors should be useful addition to the existing information. In the Indian sector, Kolkata (22.56° N, 88.36° E) was the easternmost ionosonde station nearest to the region of enhanced plasma density which operated till 1976. In the NGDC data base (http://spidr.ngdc.noaa.gov/) between Kolkata and Hainan (19.4° N, 109° E) (Singapore at 103° E, 1.3° N is at the equator), there is no ionosonde station in low-latitude region. Wichaipanich et al. (2012) reported the diurnal and seasonal variations of NmF2 in the low-latitude region over Southeast Asia. Therefore, an ionosonde in the low-latitude region of 90–100° E longitude would provide valuable measurements characterizing the most prominent peak of the longitudinal WN4 structure. The solar activity variation of low-latitude F2 layer density may get modulated by the solar activity variation of the mechanism that creates the WN4 structure. The solar cycle variation of the monthly median NmF2 has been studied extensively (Kane 1992; Sethi et al. 2002; Liu et al. 2003, 2004; Yadav et al. 2011; Liu et al. 2012, etc.) at different longitudes. Solar activity variations of daily averaged noontime NmF2 or NmF2 for multiple stations (Liu et al. 2006) or single station (Cardoso et al. 2011) have also been reported. Chen and Liu (2010) found that the rate of linear increase of monthly mean NmF2 with $F_{10.7}$ cm solar flux shows remarkable dependency on latitude, season, and local time at low solar activity levels. Walker and Ma (1972) have studied the influence of the solar flux and the equatorial electrojet on the diurnal development of the latitude distribution of the total electron content in the equatorial anomaly and reported positive correlation of electron content under the crest with electrojet. The strength of the EEJ influences the equatorial fountain and the amount and latitudinal extent of ionization transported from the equator to the lower latitudes. Rush and Richmond (1973) have studied the relationship between equatorial anomaly and the strength of the EEJ. The eastward equatorial electric field is related to the strength of EEJ (Alken et al. 2013). Deshpande et al. (1977) have reported the effect of electrojet on the total electron content of the ionosphere over the Indian subcontinent and demonstrated the association between the diurnal development of the equatorial anomaly in TEC and the electrojet strength. Earlier workers have reported positive correlation of NmF2 with EEJ in low-latitude stations in the Indian zone (Dabas et al. 1984; Dabas et al. 2006). Liu et al (2011) studied the relation of equatorial mass anomaly and EIA in the postmidnight period. Adebesin et al.

(2013) studied NmF2 and hmF2 variations with electrojet over an African equatorial station. The four peaked wave-like structure in noon time electrojet (England et al. 2006) may cause longitudinal difference in the response of the low-latitude ionosphere to electrojet. Hence, the diurnal variation of solar activity effect on daily NmF2 near the crests of the WN4 structure and the variation of the same with longitude in the context of the movement of the WN4 structure needs to be investigated. The solar cycle 24 is different from previous solar cycles like 23 or 22 in terms of level of solar activity or sunspot number and the representation in terms of solar proxies (Chen et al. 2011). During the deep solar minimum of 2007–2008, no sunspots were recorded for 266 consecutive days. The solar activity picked up very slowly in 2009–2010 and seemed to peak in June solstice of 2012 ($F_{10.7} \sim 183$). The solar activity again picked up in December solstice of 2013 to form the maximum ($F_{10.7} \sim 253$ sfu) in January 2014. The double-peak structure observed in cycle 23 (Kane 2006) is repeated in cycle 24 with much lower solar activity levels. Even at the maximum, the solar activity of cycle 24 is much less than previous cycles like cycle 23 when the highest $F_{10.7}$ flux was 325 sfu. Therefore, the investigation of solar activity variation of F2 layer parameters in solar cycle 24 may reveal new features.

In this work, we report the first time ionosonde measurements from Dibrugarh (27.5° N, 95° E, 17° N geomagnetic, 43° dip) which lies in the same longitude as the strongest daytime longitudinal enhancement (90–100° E) in density, EEJ, and vertical E × B drift, etc. (Kil et al. 2008; Lühr et al. 2008) on the northern outer edge of the equatorial anomaly. A comparison of Dibrugarh NmF2 and hmF2 data is made with that of Okinawa (26.8° N, 127° E, 17° N geomagnetic) which lies in the same geomagnetic latitude but close to the longitude of the nighttime peak in WN4 (120° E). The propagation velocity of the WN4 structure is inferred from the local time difference in the magnitude of NmF2 over Dibrugarh and Okinawa. The diurnal variation of solar activity effect on daily NmF2 and hmF2 measured over Dibrugarh and Okinawa from August 2010 till July 2014 and its seasonal variation is studied using solar activity proxies. The widely reported non-linear variation of NmF2 with solar activity (Bhuyan et al. 1983; Balan et al. 1993, 1994; Liu et al. 2006, 2007a) is shown to exhibit a diurnal variation. The correlation of Dibrugarh NmF2 and hmF2 with solar activity as well as EEJ is compared with that of Okinawa. The effect of EEJ on daily NmF2/hmF2 variations and its importance relative to solar activity is investigated. A new composite index of solar and electrodynamical activity for the low-latitude region is proposed. This index is a weighted mean of daily F10.7P and the maximum EEJ strength. The midday maximum NmF2 over Dibrugarh and Okinawa are shown to exhibit better correlation with this index than with F10.7P or EEJ. This work and the data should provide a better understanding of the physics of the low mid-latitude F2 region ionosphere along 90°E–120° E longitude.

Data and methodology

Canadian Advanced Digital Ionosonde (CADI) was installed in Dibrugarh in July 2010. CADI is a modern low-power digital ionosonde of peak power of around 650 W and frequency range of 1–20 MHz. The transmitter antenna is an inverted delta type. The length of the antenna is around 59 m, and it is supported on a 15-m-high tower. The receiver antenna system consists of four dipole receivers of 30 m each arranged in rectangular geometry. The operation of the ionosonde is automated and the ionograms every 10/15 min are recorded in 24 × 7 mode.

The hourly averaged F2 layer critical frequency foF2 and the F2 layer real height hmF2 measured by the ionosonde for the quiet days of the period of August 2010 till July 2014 are used in this study. This is the ascending phase of solar cycle 24. The solar activity ($F_{10.7}$ cm flux) variation for this period is shown in Fig. 1. We note that the solar activity even during the maximum of the cycle is not quite high and may be termed as moderately high only. NmF2 is calculated from manually scaled values of foF2 by using the formula $NmF2 = 1.24 \times (foF2 \text{ in MHz})^2 \times 10^{10}$ per cubic meter for the quiet days ($Kp < 3$) of the month. The hmF2 values for Dibrugarh are obtained from the true height profile generated by inversion of ionograms using POLAN (Titheridge 1985) for the ten quietest days of the month given in Kyoto University geomagnetic data service website (http://wdc.kugi.kyoto-u.ac.jp/). The NmF2 and hmF2 data for Okinawa was obtained from the National Geophysical Data Center (NGDC) web site http://spidr.ngdc.noaa.gov/. F10.7P and the solar extreme ultraviolet (EUV) flux measured by the Solar EUV Monitor (SEM) of Solar Heliospheric Observatory (SOHO) are used as indicators of solar flux variation. Here, $F10.7P = (F_{10.7} + F_{10.7}A)/2$ and $F_{10.7}A$ is the 81-day running mean of $F_{10.7}$. For estimating the equatorial electrojet, the earth's magnetic field H at the pair of stations located on and off the equator is measured. Following Chandra and Rastogi (1974), the strength of the Electrojet is estimated as

$$\Delta H = H_{\text{eq}} - H_{\text{off equator}}$$

where H_{eq} is the horizontal component of the earth's magnetic field at the equatorial station and $H_{\text{off equator}}$ is the H component at an off-equatorial station. The station pair for the Indian zone is Tirunelveli (0°)-Alibag (23° N), and the data period is August 2010–December 2012. The station pair for Okinawa is Davo (1° S)-

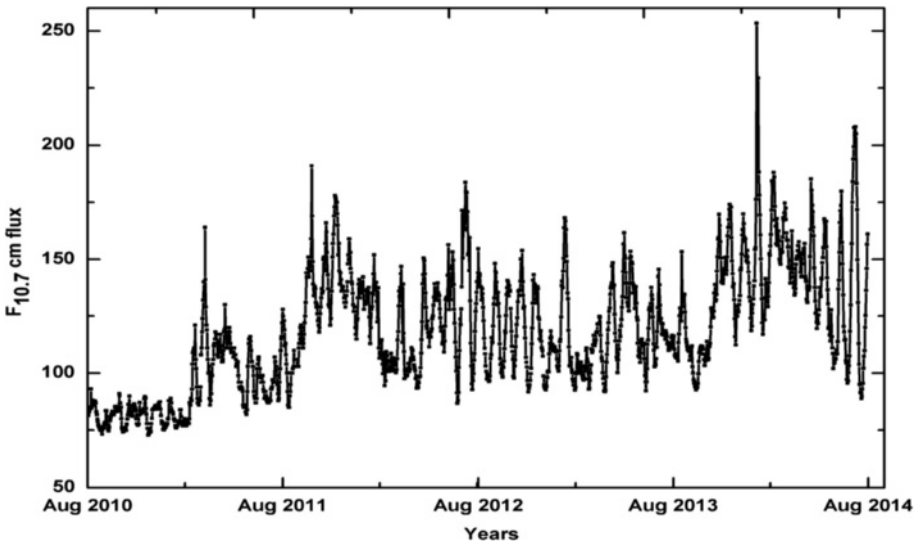

Fig. 1 $F_{10.7}$ index from August 2010 to May 2014

Muntinlupa (7° N), and the data period is August 2010–April 2014. The neutral parameters and ion temperature are obtained from the NRLMSISE and IRI models, respectively.

Results and discussion

Diurnal and seasonal variations of NmF2

The seasonal variation of NmF2 is illustrated as a function of local time in Fig. 2 for low solar activity (August 2010–August 2011) and moderately high solar activity (September 2011–July 2014), respectively. The NmF2 is highest in equinox and lowest in December (June solstice) solstice for low (high) solar activity conditions. Nighttime NmF2 is higher in March equinox and June solstice. In low solar activity period, the diurnal maximum is observed around 1300–1400 LT in December solstice, 1400–1500 LT in equinox, and 1500–1600 LT in June solstice. In high solar activity period, the time of occurrence of the diurnal maximum for December solstice is delayed by about 1 h whereas for other seasons, the time of occurrence remains the same. This indicates a reduction in December solstice to June solstice delay in the occurrence of the daytime peak. In both low and high solar activity conditions, equinoctial asymmetry is observed, i.e., NmF2 is higher in March equinox than in September equinox. Equinoctial asymmetry has been reported earlier by Titheridge (1973), Da Rosa et al. (1973), Essex (1977), Balan and Otsuka (1998), Chen et al. (2012) and Ren et al. (2014). To delineate the seasonal variation of NmF2 from the variation of NmF2 due to solar activity, the NmF2 dataset (August 2010–May 2014) was detrended using the following procedure. The second order fitting of daily NmF2 values with the corresponding daily values of solar activity proxy F10.7P is used to obtain the trend of variation with solar activity. The NmF2 value predicted by the fitted curve for a particular solar flux level is subtracted from the observed NmF2 to obtain the detrended NmF2. The time series of detrended NmF2 is shown in Fig. 3. A semi-annual variation in daytime maximum density of the F2 layer is clearly observed with the two peaks occurring in the equinoxes. The peak in March equinox is higher than the peak in September equinox. The asymmetry of the thermospheric O/N_2 ratio may have contributed to the equinoctial asymmetry (Hazarika and Bhuyan 2014). Bhuyan and Hazarika (2012) have observed the winter anomaly in TEC only in the high activity period of 2011–2012 over the same location and attributed this to the change in the thermospheric O/N_2 ratio as observed from GUVI satellite. From Fig. 2a,b, it is observed that in low solar activity period of 2010–2011, the seasonal average NmF2 is higher in June solstice than that in December solstice whereas in the high solar activity period of 2012–2014, the seasonal average NmF2 in December solstice and June solstice are of the same order with June solstice NmF2 slightly on the lower side. Therefore, a weak winter anomaly in midday NmF2 can be observed over Dibrugarh during high solar activity period of 2012–2014, but no winter anomaly is observed in the low solar activity period of 2010–2011. The weak winter anomaly could be due to the decreasing trend of solar flux from the second half of 2012 to September equinox of 2013 leading to a double peak in solar cycle 24 or lower level of activity during this cycle. To confirm this hypothesis, we investigated the seasonal NmF2 variation in June solstice and December solstice of 2010–2011, 2011–2012, 2012–2013, and 2013–2014 separately in Fig. 4. The winter anomaly in forenoon and midday NmF2 can be clearly observed during 2011–2012 and 2013–2014 whereas it is

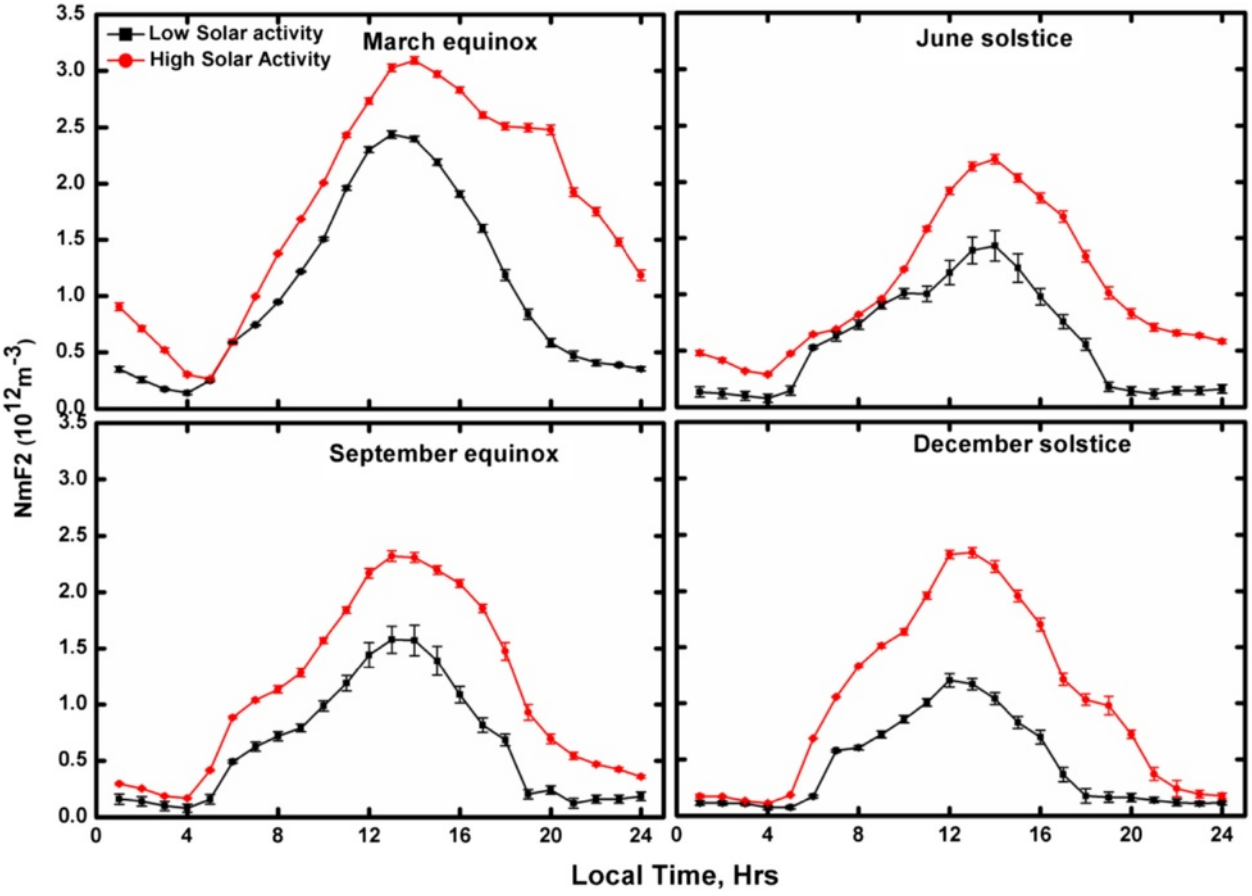

Fig. 2 The seasonal variation of NmF2 in low solar activity period of August 2010–August 2011 and high solar activity period of September 2011–July 2014. The *error bars* indicate the standard deviation of the data

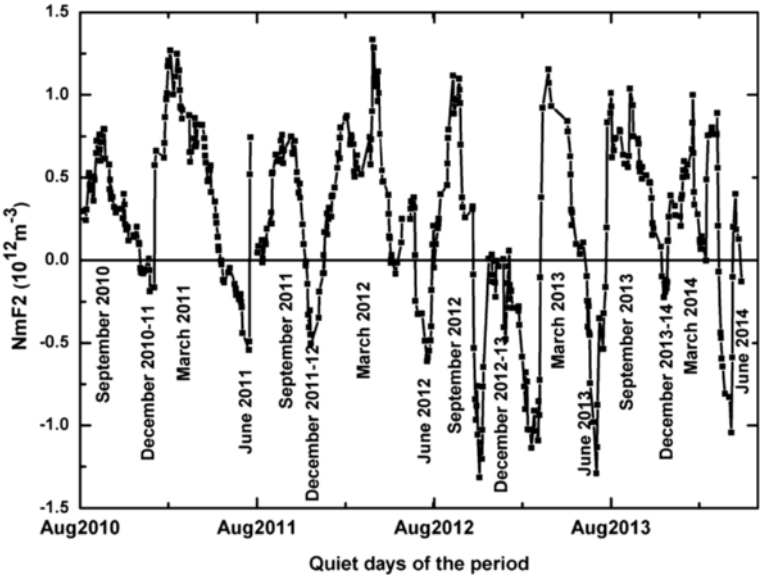

Fig. 3 Detrended seasonal variation of NmF2 for the period of August 2010–April 2014

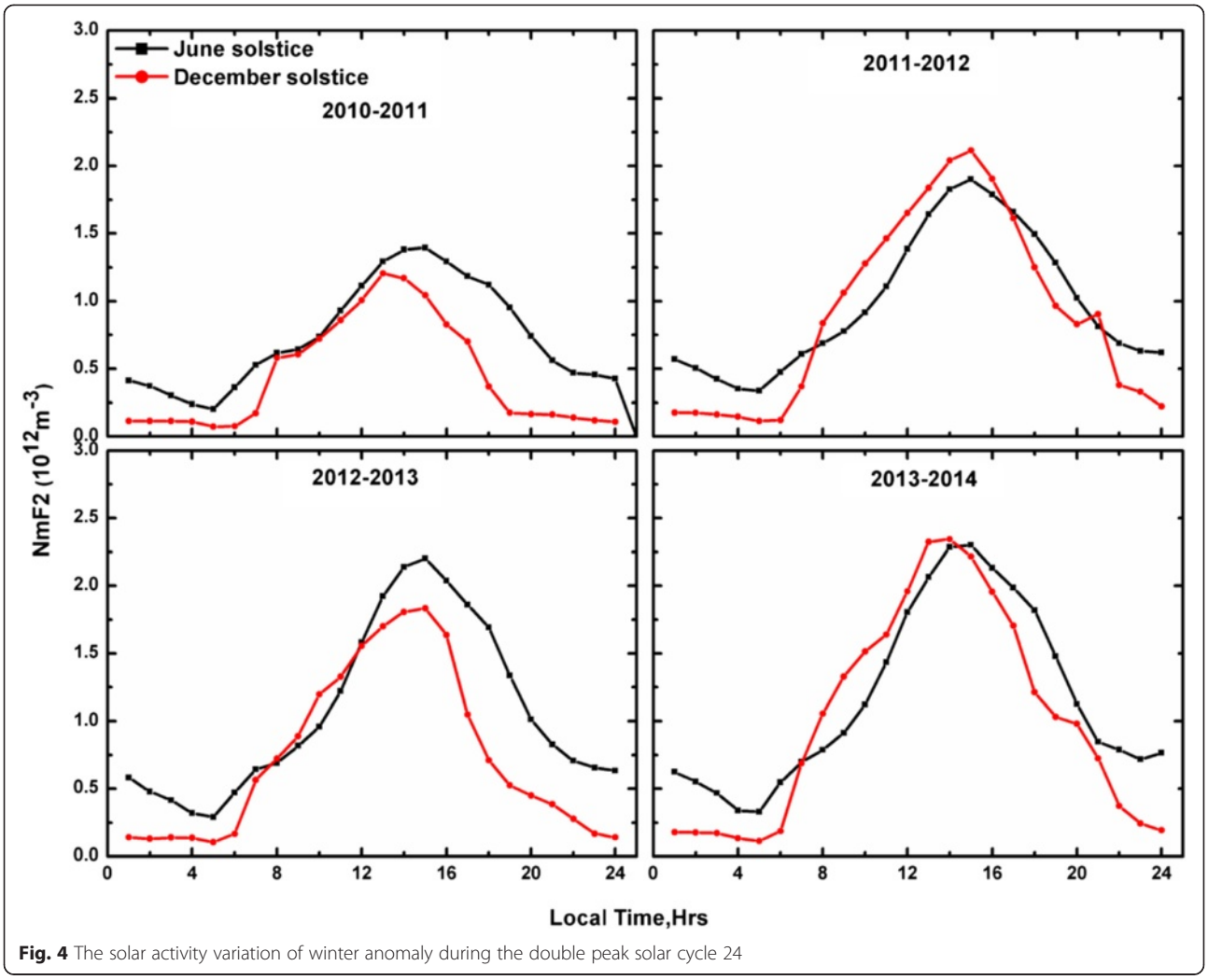

Fig. 4 The solar activity variation of winter anomaly during the double peak solar cycle 24

present only during a couple of forenoon hours during 2012–2013. The dip in solar activity during 2013 is manifested in temporary disappearance of the midday winter anomaly over Dibrugarh. Therefore, the effect of solar activity on NmF2 is stronger in the forenoon than that in the midday period. The rate of increase of NmF2 in the forenoon hours of high solar activity hours is fastest as compared to the other daytime hours and may be related to the more pronounced winter anomaly in the forenoon period. The local time variation of $[O]/[N_2]$ ratio at the altitude of the F2 layer may be related to the local time dependence of the winter anomaly. The local time effect on NmF2 solar activity variations is discussed further in the "The variation of NmF2 with solar activity" section.

Diurnal and seasonal variations of NmF2 over Okinawa

The longitudinal WN4 structure peak in electron density maximizes around 90°–100° E during daytime and around 120° E at nighttime. The WN4 structure is postulated to be related to the non-migrating eastward propagating diurnal tides (Immel et al. 2006) as it evolves with local time and moves eastward (Lin et al 2007b; Scherliess et al. 2008; Fang et al. 2009). Therefore, comparison of simultaneous ground measurements (NmF2/hmF2) in these longitude sectors (90–120° E) might complement the earlier observation from satellites and reveal new features. The pair of ionosonde stations at Dibrugarh (27.5° N, 95° E, 17° N geomagnetic) and Okinawa (26.5° N, 127° E, 17° N geomagnetic) provide the opportunity of comparing the NmF2 at these longitudes as they are virtually at the daytime and nighttime peak of the WN4 structure and also at the same geomagnetic latitude. Simultaneous measurements at the two stations are available from 2010 to 2014.

The diurnal variation of NmF2 in these two stations for the four seasons is shown in Fig. 5 for low solar activity conditions (August 2010–August 2011) and moderately high solar activity conditions (September 2011–April 2014). The diurnal variation of NmF2 over Dibrugarh and

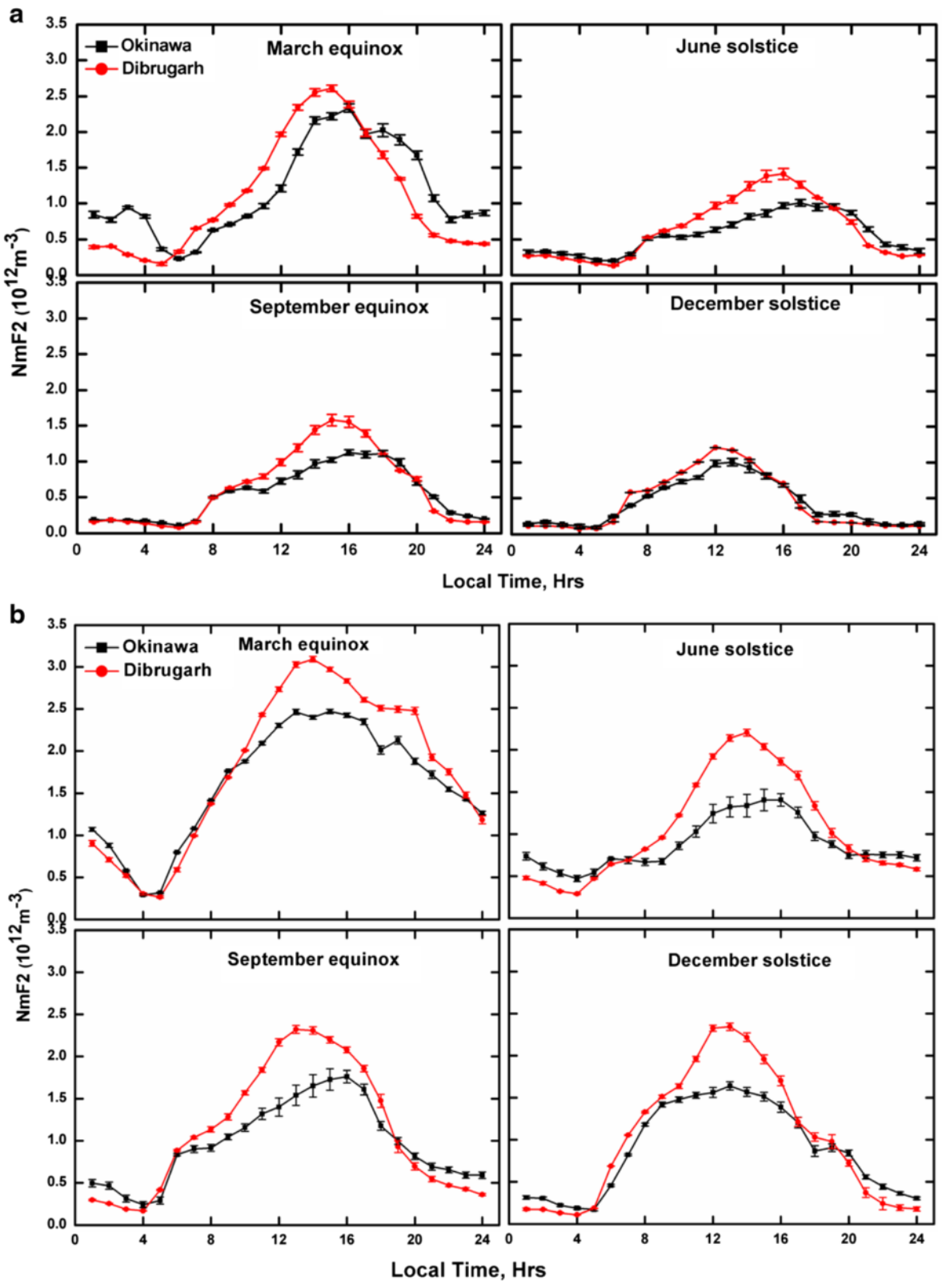

Fig. 5 The seasonal variation of NmF2 over Dibrugarh and Okinawa for **a** low (August 2010–August 2011) and **b** high solar activity (September 2011–April 2014). The *error bars* indicate the standard deviation of the data

Okinawa are similar in December solstice but significantly different in equinox and June solstice of low solar activity period. The daytime NmF2 over Dibrugarh are found to be much higher than that of Okinawa in these three seasons. The diurnal peak of NmF2 in Dibrugarh is obtained slightly earlier as compared to that of Okinawa, particularly in low solar activity June solstice and September equinox. In all seasons, NmF2 in Dibrugarh decreases to level below that of Okinawa in the nighttime. In the high solar activity period, June solstice and September equinox NmF2 variations are similar to those during low solar activity. In December solstice and March equinox of the same period, postsunset enhancement in NmF2 (Rao 1963b) is observed which may be related to the stronger pre-reversal enhancement (PRE) in high solar activity (Fejer et al. 1979). In this period, the difference between Dibrugarh and Okinawa becomes appreciable in December solstice. In general, the magnitude of NmF2 over Dibrugarh is higher in the daytime and lower in the nighttime than that of Okinawa. An inspection of the diurnal development of NmF2 reveals that in the early morning period, the NmF2 over Dibrugarh and Okinawa have nearly the same values. The NmF2 over Dibrugarh starts increasing at a faster rate from around 0700 LT when the WN4 structure is reported to develop and is significantly higher than the NmF2 over Okinawa by 1400–1500 LT when the WN4 structure is fully developed. In contrast, the NmF2 over Okinawa increases at a relatively slower rate in the morning and the diurnal maximum is observed after 1600 LT in September equinox and June solstice of low solar activity period. A plateau is formed thereafter, and the NmF2 starts to decay around 1900–2000 LT whereas the NmF2 over Dibrugarh falls rapidly after 1600 LT. From evening to early morning period, the NmF2 over Dibrugarh decays at a faster rate and becomes lower than that of Okinawa. In high solar activity period of 2012–2014 (Fig. 5b), the NmF2 over Dibrugarh remains higher than that over Okinawa till late evening hours. This is particularly true for June solstice and March equinox. For quantitative study, the average difference in hourly NmF2 between the two stations is plotted against local time in Fig. 6. During low solar activity, the maximum difference in NmF2 between Dibrugarh and Okinawa ($\Delta NmF2 = NmF2_{dib} - NmF2_{oki} > 8 \times 10^{11}/m^3$) is observed in the midday (1200–1300 LT) and the late evening period (2000 LT) of equinox whereas minimum difference is observed in the early morning period (0800 LT) and sunset period (1700–1800 LT). The daytime peak in ΔNmF2 is weakest in December solstice but nighttime peak is weakest in June solstice. The absence or weak WN4 peak at 120° E during June solstice (Liu and Watanabe 2008) could result in weaker nighttime peak in June solstice. During high solar activity, the maximum difference between Dibrugarh and Okinawa is observed in June solstice ($\Delta NmF2 = NmF2_{dib} - NmF2_{oki} \sim 9 \times 10^{11}/m^3$) around 1300 LT. The difference between the two stations increases in December solstice when solar activity increases. The trend is clearly of higher values over Dibrugarh in the daytime and higher values over Okinawa in the nighttime with the transition taking place during the early morning and sunset periods. The difference in NmF2 increases gradually in low solar activity solstice as compared to equinox in the daytime to reach the maximum in the midday period (later in September equinox and solstices as compared to March equinox) and then decays rapidly to change the phase during sunset. The nighttime peak in ΔNmF2 also exhibits similar development with the phase change taking place in the postsunrise period. The wavelike structure of the hourly NmF2 is most probably related to the eastward movement of the WN4 structure from 95° E to 127° E. The seasonal variation of the ΔNmF2 notably the minimum difference in December solstice and the timing of maxima and phase change (morning and sunset periods) are consistent with the behaviour of the WN4 structure (Liu and Watanabe 2008; Jin et al 2008; Ren et al. 2009). The average time difference between the daytime and nighttime peak in ΔNmF2 is about 7–8 h in low solar activity period and about 10 h in high solar activity period. The time lag between the two maxima in ΔNmF2 can be used to estimate the propagation speed for the WN4 assuming that the local time of the two maxima corresponds to longitudinal position of the WN4 peak. The propagation speed of the WN4 structure estimated by this method is about 4.3°/h in low solar activity and about 3.2°/h in high solar activity. The speeds are higher in the low solar activity and lower in the high solar activity. The propagation speed in the high solar activity is of the same order as those estimated by Jin et al. (2008) for daytime hours. The estimated speeds in this study differ from the theoretical speed (3.75°/h) of the WN4 structure by about 15 %. The difference could be partly due to the use of hourly averaged NmF2. The solar activity variation of the estimated speeds could be due to the solar activity variation of the location and the strength of the WN4 peaks (Liu and Watanabe 2008). Considering the similar local time, seasonal, and solar cycle variations of the longitudinal WN4 structure and the hourly ΔNmF2, we suggest that the observed NmF2 difference between Dibrugarh and Okinawa is due to the longitudinal WN4 structure in electron density and we further validate the result by showing that the propagation speed of the WN4 structure estimated from the ground measurements is close to the theoretical value.

The variation of NmF2 with solar activity

It was observed that during the period of study which corresponds to the rising and peak activity period of solar cycle 24, the daily noon time maximum NmF2 over Dibrugarh is not well correlated with solar activity proxy

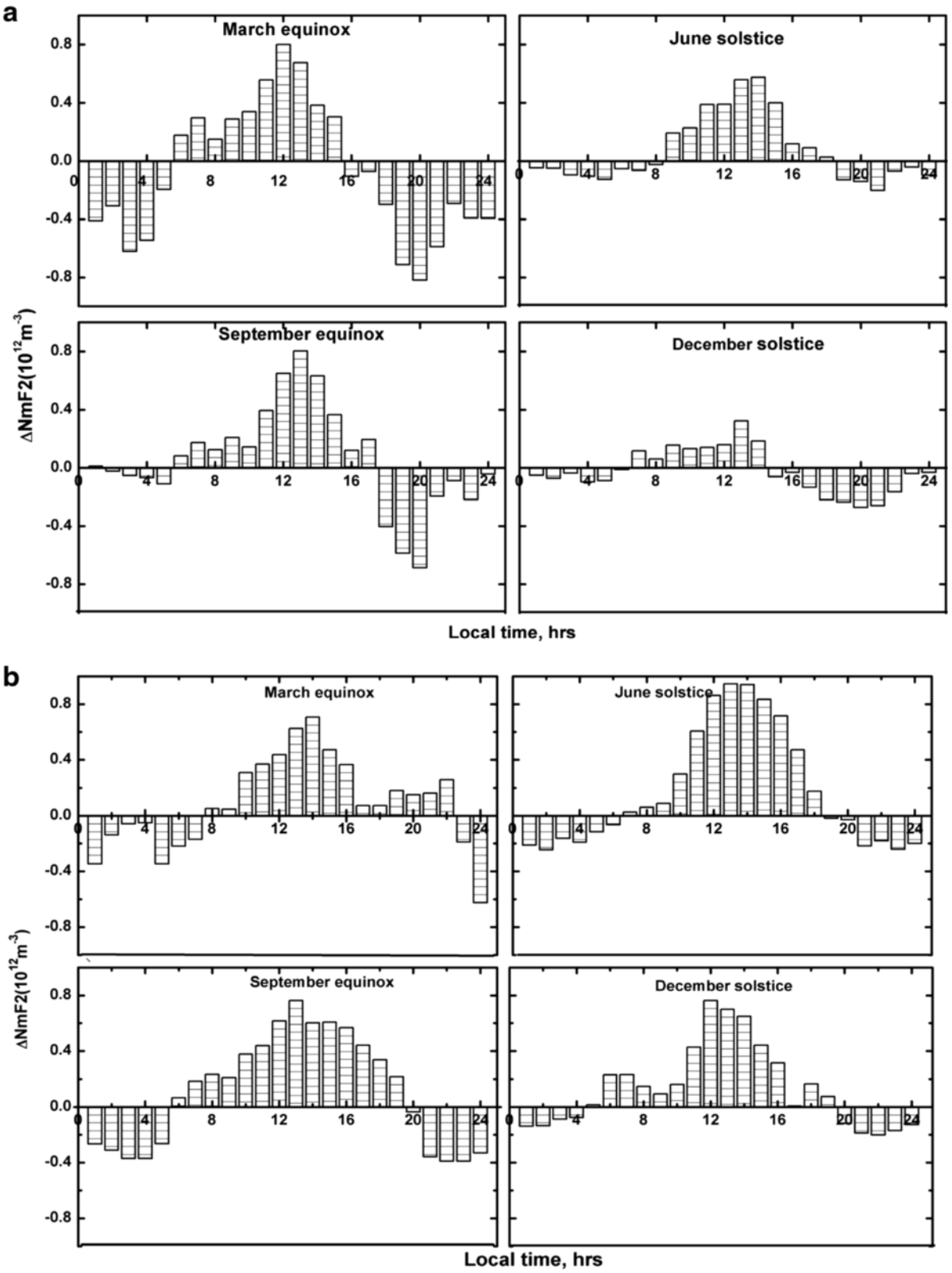

Fig. 6 The average hourly variation in ΔNmF2 ($NmF2_{Dibrugarh} - NmF2_{Okinawa}$) for **a** low and **b** high solar activity conditions

F10.7P or solar EUV flux measured by SOHO/SEM ($r < 0.5$, not shown here) whereas over Okinawa, the daily maximum NmF2 is better correlated ($r \sim 0.55$) to solar activity. Detailed investigation of hourly NmF2 revealed that the correlation of NmF2 with the solar activity indices exhibited a diurnal variation, and the best correlation is observed in the forenoon hours. The variation of daily 1000 LT NmF2 with F10.7P and Solar EUV flux for geomagnetically quiet days is shown in Fig. 7. We observe that the correlation improves marginally for non-linear fitting with solar EUV flux. The correlation of the forenoon NmF2 is higher over Dibrugarh as compared to that of Okinawa. For both stations, the highest and lowest correlations are observed in March equinox and June solstice, respectively (not shown). Seasonal variation of the equatorial anomaly, the WN4 structure, and global thermospheric composition and circulation may account for the observed seasonal variation. To examine the non-linear variation of NmF2 with solar activity, the daily NmF2 variations at different hours are fitted with a second-order polynomial shown in Eq. 1 below.

$$N = a_2 x^2 + a_1 x + a_0 \quad (1)$$

Here, N is hourly NmF2, x is solar EUV flux, and a_2 and a_1 are the first- and second-order coefficients. Improvement in correlation is observed depending on local time and season. The correlation of maximum daytime NmF2 over Dibrugarh with F10.7P is poor ($r < 0.5$) even in the case of second-order fitting, and the saturation effect is very weak (not shown). Bhuyan and Hazarika (2012) observed the saturation effect in maximum daytime TEC measured over Dibrugarh with daily $F_{10.7}$ cm flux. The apparent difference in the response of TEC and NmF2 could be due to three factors: (1) different solar activity index used, (2) different data period, and (3) different physical mechanism around the F2 layer peak and the topside. Bhuyan and Hazarika (2012)

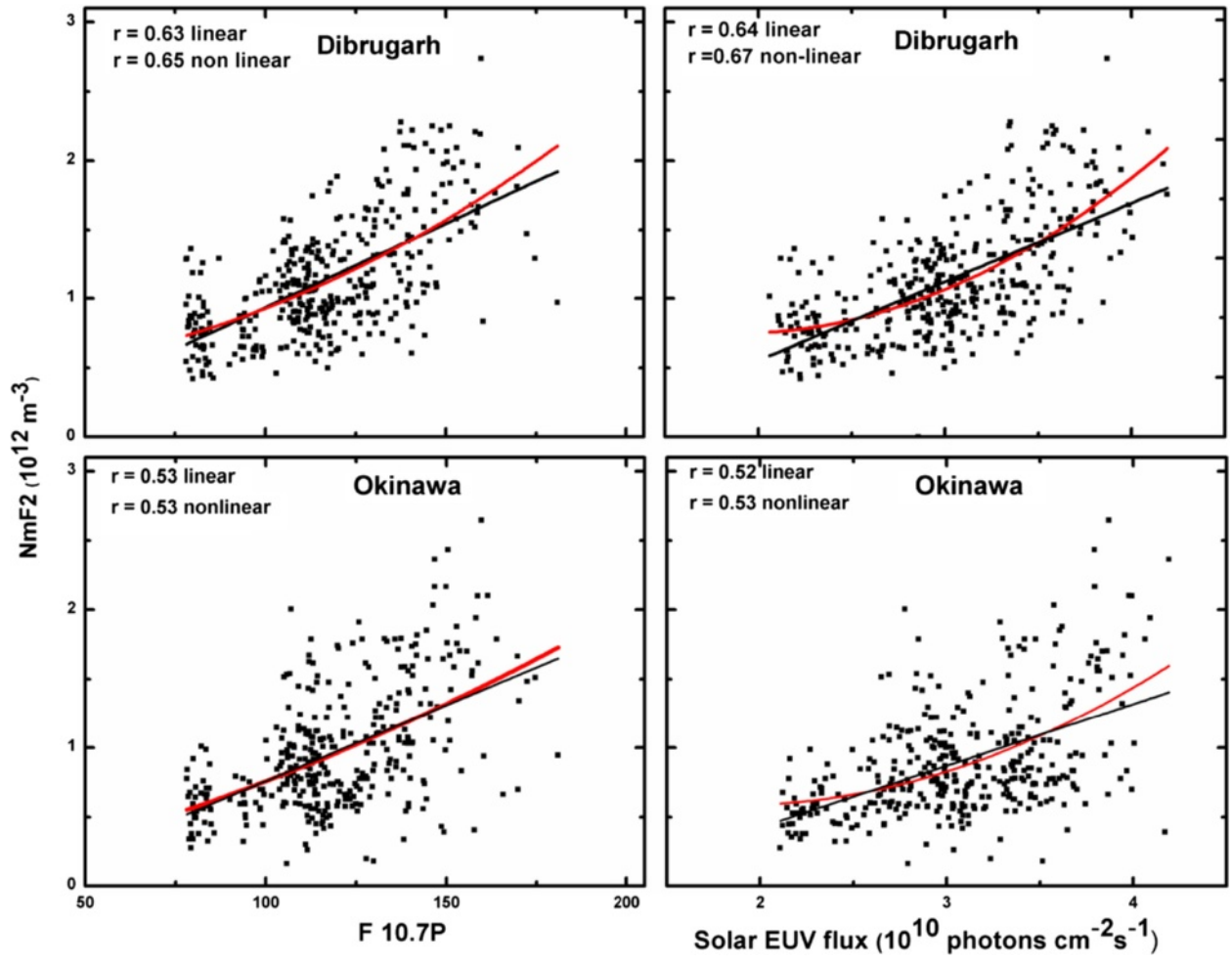

Fig. 7 The scatter plot showing the variation of 1000 LT NmF2 over Dibrugarh and Okinawa with F10.7P and solar EUV flux

studied the TEC variation with daily $F_{10.7}$ cm flux for the period 2009–2012 whereas in this study, we have used the modified index F10.7P and solar EUV flux measured by SOHO/SEM for the period 2010–2014. Therefore, the saturation effect observed by Bhuyan and Hazarika (2012) with $F_{10.7}$ may be due to the non-linear variation of $F_{10.7}$ cm flux with solar EUV flux in the high solar activity period as pointed out by Balan et al. (1994). Additionally, the TEC represents the vertically integrated density of the ionosphere which include the topside as well as the bottom side density whereas NmF2 is obtained from the measurement of the bottom side of the F2 layer. The TEC is affected by the physics of the topside where diffusion and the electrodynamics and in particular the transport due to equatorial fountain effect via the E × B drift are dominant factors in low-latitude region. The effect of solar activity on electron density varies with altitude (Su and Bailey 1999), and depending on altitude and season, the topside density can exhibit linear, saturation, and amplification trend with solar activity (Liu et al. 2007; Chen et al. 2009). NmF2 is the highest density of the F2 layer, and the altitude of the highest density hmF2 varies with local time, season, solar cycle, and magnetic activity. The variations of hmF2 affect the solar activity variations of NmF2 (Liu et al. 2006). Therefore, the response of the TEC and the NmF2 to solar activity may be different, particularly in terms of the threshold levels for onset of the saturation effect.

The coefficient a_2 in Eq. 1 represents the non-linearity of the fitted curve, and its sign indicates whether NmF2 is saturated ($a_2 < 0$) or amplified ($a_2 > 0$) with solar activity. In Fig. 7, the tendency for non-linear variation of NmF2 with solar EUV flux was observed at 1000 LT and, therefore, we examined the nature of the NmF2 variation trend at each hour of the day with F10.7P and EUV flux. It was found that the same hourly data set which tends to saturate with F10.7P increases linearly with solar EUV flux. Similarly, the dataset which increases linearly with F10.7P shows the amplification effect with EUV flux. Therefore, we find a non-linear relation between F10.7P and solar EUV flux and confirm that the ionospheric response to solar activity is affected by the non-linear relationship between solar activity indices (Balan et al. 1993). The diurnal and seasonal variations of the coefficient a_2 with solar EUV flux measured by SHOHO/SEM are shown in Fig. 8. In both the stations, the value of a_2 is generally higher in the forenoon and postsunset periods as compared to that in the midday period. There are subtle differences in the seasonal variation of a_2. In March equinox, positive values of a_2

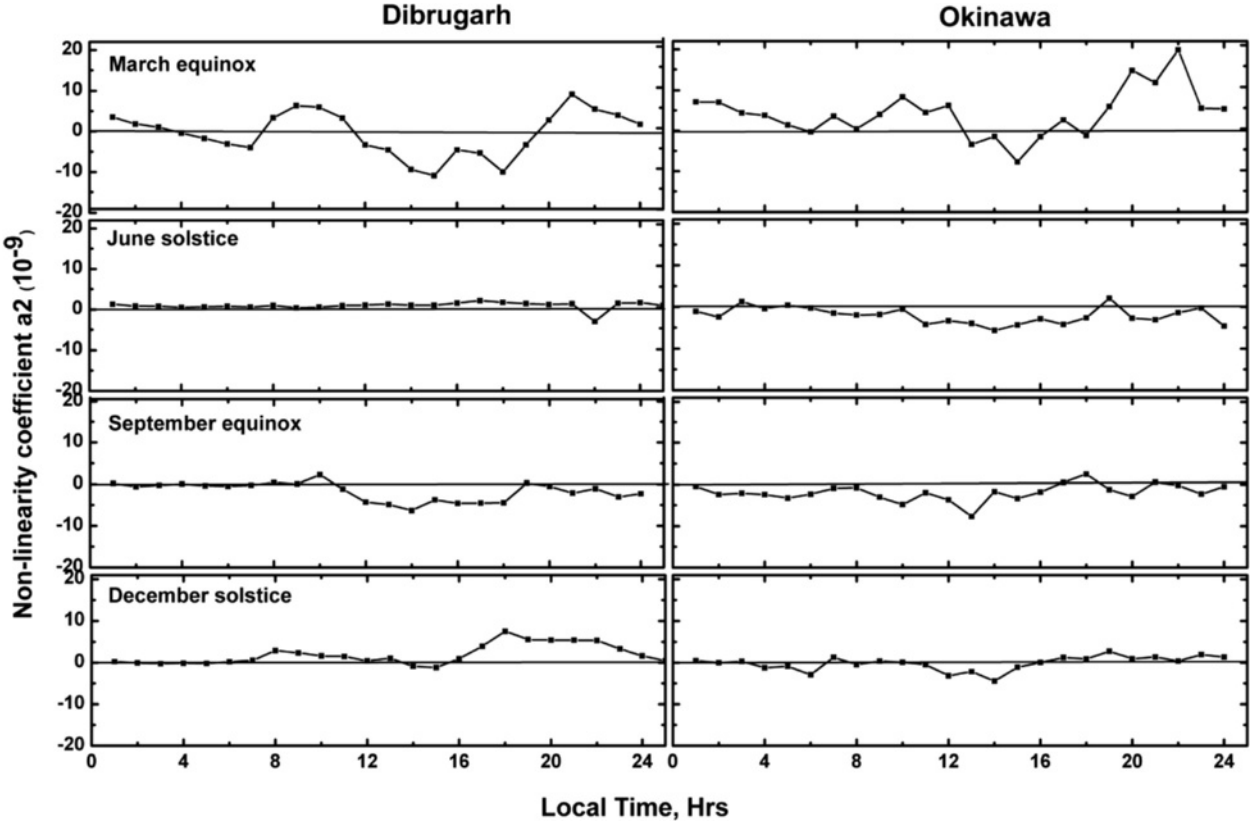

Fig. 8 The diurnal and seasonal variations of non-linearity coefficient a_2 obtained between NmF2 and solar EUV flux over Dibrugarh and Okinawa

are seen in the forenoon and the pre-midnight period signifying a weak tendency for amplification. Negative a_2 in the midday period hints at the saturation effect. In June solstice, a_2 remains close to zero throughout the day in the case of Dibrugarh, suggesting a linear increase of NmF2 with solar activity. In the case of Okinawa, the slight negative bias in a_2 except for a brief period in the morning of June solstice suggests weak saturation effect in NmF2. In September equinox, a_2 is negative in the midday which suggests that NmF2 is more likely to saturate in high solar activity. In the forenoon period of December solstice, a_2 is weakly positive but in the postsunset period, a_2 is clearly positive over Dibrugarh but weakly positive over Okinawa. Therefore, in the forenoon and postsunset periods, the NmF2 increases linearly in June solstices and September equinox but there is a tendency for amplification in March equinox and December solstice. In the case of Dibrugarh, the NmF2 may exhibit the saturation effect only in the midday period of equinox. The latitudinal variation of the location of the EIA crest relative to Dibrugarh and Okinawa and the movement of the EIA crest towards higher latitudes (Bhuyan et al. 2003) in equinox may account for such seasonal differences as the saturation effect is most pronounced in the EIA region (Ma et al. 2009; Liu et al. 2003). The non-linear variation as indicated by a_2 can at best be termed as tendency for non-linear variation due to moderately high level of solar activity in solar cycle 24. Our observation of the nighttime amplification effect in Dibrugarh and Okinawa (*low* mid-latitude stations) in December solstice is consistent with Chen et al. (2008) where they have reported the amplification effect in nighttime NmF2 in December solstice for low- and mid-latitude region. Most of the earlier workers (Liu et al. 2003; Ikubanni and Adeniyi 2013) have reported only the saturation effect in daytime NmF2 over low-latitude region. Ma et al. (2009) reported non-linear increasing (amplification) effect for mid- and high latitudes only. Chen and Liu (2010) also reported the likelihood of the amplification effect in the early morning sector for mid-latitude stations in March equinox. In this study, we have observed a tendency for non-linear increase or amplification of NmF2 in the forenoon and premidnight periods of March equinox. The result suggests that these two stations located in the transition region between low- and mid-latitudes may exhibit mid-latitude like behavior in the forenoon period before the full development and extension of the EIA to higher latitudes in the afternoon. In the midday period, the crest of the anomaly moves closer to Dibrugarh and Okinawa and low-latitude-like behavior is more likely. Therefore, the local time variation in the NmF2 solar activity trends may be related to the location of the two stations.

To interpret these local time and seasonal variation of solar activity trends, we discuss various factors influencing the electron density in low- and mid-latitude region. The daytime electron density is determined by the balance of production due to photoionization, recombination loss, and transport (Rishbeth and Garriot 1969). In addition to the effect of neutral dynamics, the transport due to equatorial fountain effect influences the midday electron density in low-latitude region near the anomaly crest. The equatorial anomaly starts to develop in the morning around 0900 LT but the crest in this period is closer to the equator (Sastri 1990). The anomaly reaches its peak strength during the postnoon period (1300–1600 LT) after a time lag of around 2–3 h from the time of the maximum electrojet strength (Rush and Richmond 1973). Therefore, the contribution of the transport process via fountain effect to the enhancement of NmF2 in the low-latitude region is less significant in the forenoon hours than in the midday hours. The E × B vertical drift which peaks around 1100 LT (Fejer et al. 1979; 2008) in the daytime low-latitude region can affect the density at a particular altitude but the daytime E × B vertical drift is almost the same for low and high solar flux conditions (Scherliess and Fejer 1999; Fejer et al. 2008). The variation of F2 layer height (hmF2) may also affect the variation trends of NmF2 with solar activity through the altitudinal dependency of solar activity effect (Su and Bailey 1999). In the forenoon period, the electron density in low mid-latitude stations like Dibrugarh/Okinawa would be mainly affected by the production-loss mechanism and the neutral dynamics. Therefore, the diurnal, seasonal, altitudinal, and solar activity variations of neutral composition, chemical reactions rates, and dynamics would affect the observed diurnal and seasonal variations of NmF2 solar activity effect.

The solar activity variation of neutral gas constituents as obtained from NRLMSISE model at the seasonally averaged height of F2 layer were examined for the period of study (2010–2014). Atomic oxygen O is the dominant constituent in the altitude range of the F2 layer peak density, and its concentration influences the production of ionization the most. Therefore, only the solar activity variation of the forenoon (1000 LT) concentration of atomic oxygen [O] (as representative of neutral composition) over Dibrugarh at the altitude of F2 layer for March equinox and September equinox conditions is shown in Fig. 9. The [O] increases non-linearly in March equinox and linearly in September equinox with solar EUV flux for the solar activity range of this study ($F_{10.7}$ ~ 80–160 sfu, EUV ~ (2–4.5) E + 10 photons cm^2 s^1). The [O] in March equinox increases slowly from low to moderate solar activity and increases at a relatively faster rate for moderate to high solar activity. The [O] seems to vary linearly in September equinox where the forenoon

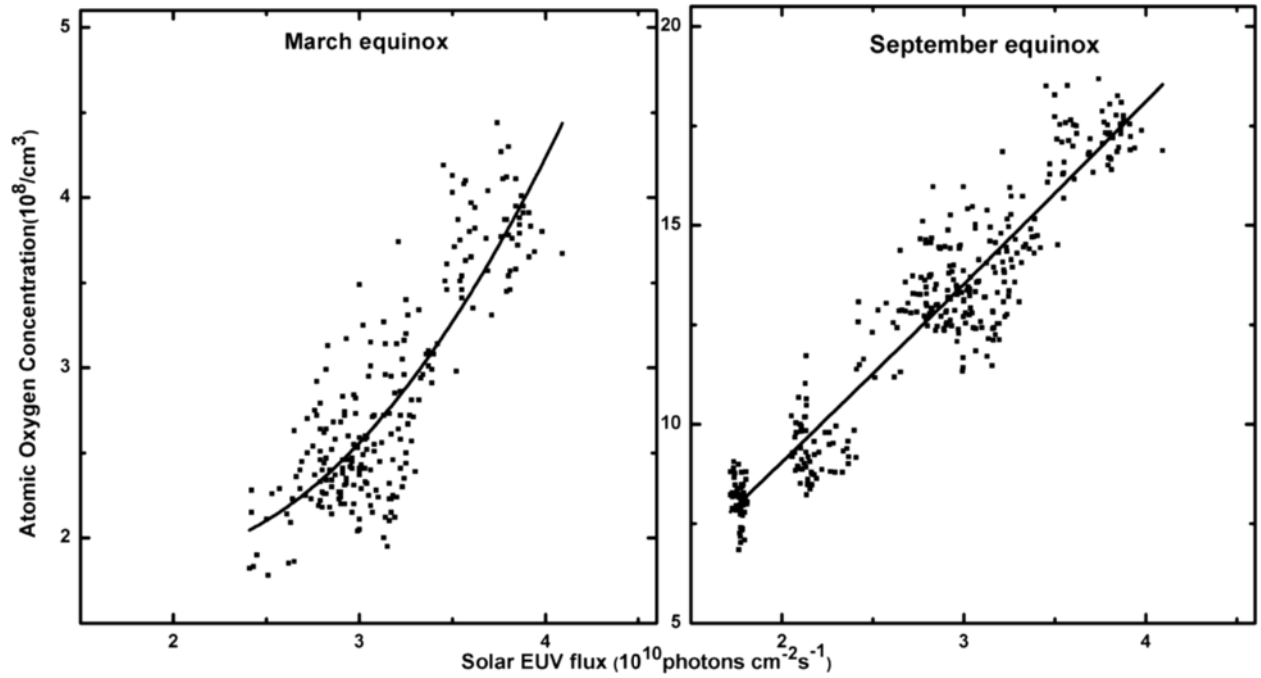

Fig. 9 The scatter plot showing the solar activity variation of forenoon atomic oxygen concentration over Dibrugarh obtained from NRLMSISE model during August 2010–July, 2014

averaged hmF2 varies from 270 to 320 km ("The diurnal and seasonal variations of hmF2 at Dibrugarh and Okinawa" section) with solar activity and non-linearly in March equinox where the forenoon averaged hmF2 varies from 325 to 370 km with solar activity. The amplification tendency in the forenoon period of March equinox and its absence in September equinox may be related to the altitudinal difference of solar activity effect on atomic oxygen concentration. The [O] was found to increase linearly in the solstices. Therefore, the faster buildup of [O] during high solar activity March equinox would increase NmF2 faster due to increased production. The local time variation of $[O]/[N_2]$ ratio at the altitude of F2 layer also shows a peak in the forenoon period of March equinox for low mid-latitude region (Chen and Liu 2010). The non-linear increase of [O] with solar activity is also observed in the midday period-afternoon period (not shown), but in the midday period, only linear (solstice) or saturation (equinox) trend of NmF2 is observed over Dibrugarh. The local time variation of $[O]/[N_2]$ and the thermospheric temperature may be related to the different trends in NmF2 in the forenoon and the afternoon periods. Higher temperature in the midday would raise molecular neutral density at F2 layer height thereby increasing the recombination loss. Therefore, in addition to neutral composition, the loss due to recombination also needs to be investigated for solar activity dependence. The electron density is lost through chemical recombination process mainly via the following two reactions:

$$O^+ + N_2 \rightarrow NO^+ + N$$
$$O^+ + O_2 \rightarrow O_2^+ + O$$

The reaction rates for these two process decreases with increase in effective temperature $T_F((7Ti + 4Tn/11)$ for temperature lower than 1100 K (Hierl et al. 1997; Su and Bailey 1999). The rate of the first equation reverses trend and starts increasing, and the rate of the second equation becomes almost constant as temperature increases beyond 1100 K. Figure 10 shows the variation of effective temperature with solar activity for the period of 2010–2014 in the forenoon (1000 LT) and afternoon periods (1600 LT), respectively. The neutral and ion temperature are obtained from NRLMSISE and IRI, respectively. The effective temperature in the forenoon period increases with solar activity but remains below 1100 K, whereas in the midday-afternoon period, it shoots past 1100 K when solar activity is high. Therefore, when solar activity increases, the chemical reaction rates and loss due to recombination would be reduced in the forenoon hours but enhanced in the afternoon period. The reduction of recombination loss rate with the increase in solar activity would help to increase the NmF2 in the forenoon hours. Therefore, the decreasing loss rates along with non-linear increase (amplification) of neutral composition with solar activity could contribute to the amplification trend of forenoon NmF2 from low to moderately high solar activity condition during 2010–2014. The reverse case of increased loss rate in the postnoon period could contribute to midday saturation effect

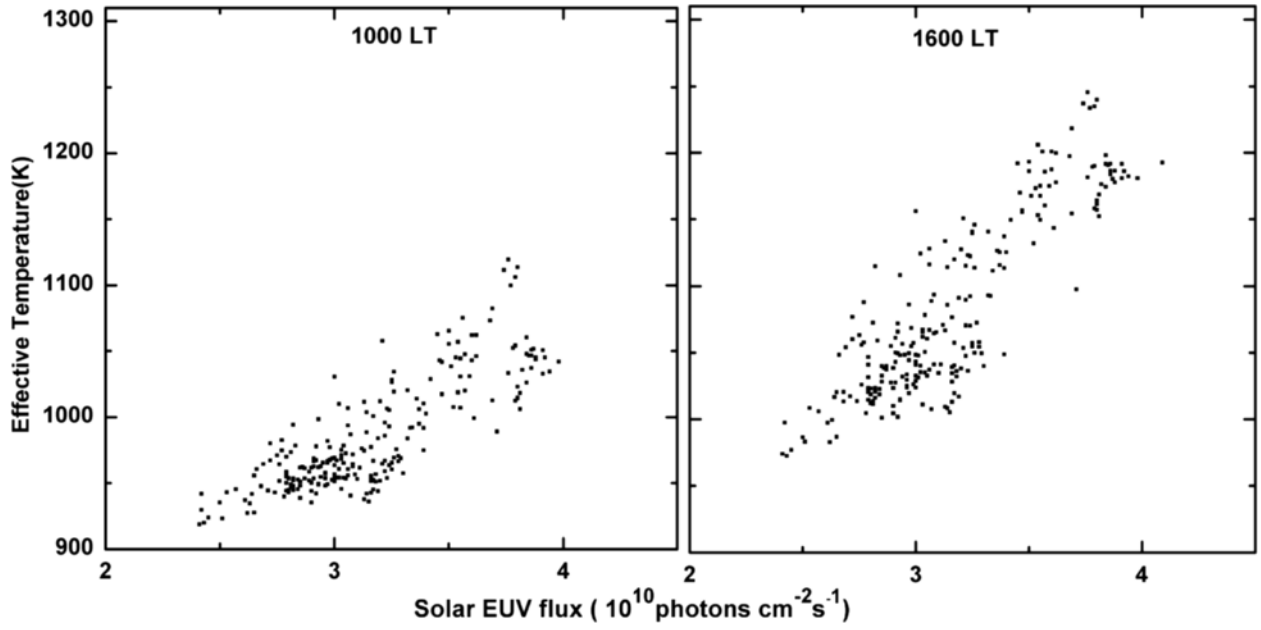

Fig. 10 The scatter plot showing the solar activity variation of effective temperature over Dibrugarh at 1000 LT and 1600 LT calculated with inputs from NRLMSISE and IRI model during the period of August 2010–July 2014

in NmF2. Mikhailov and Perrone (2011) have also attributed the variation of recombination loss coefficient via temperature dependence as the cause of non-linear variation of NmF2 in mid-latitude region. If the solar activity is higher than 160 sfu (as in previous cycles like 23/22), the rate of increase of neutral parameters with solar activity decreases in the high solar activity end (Su and Bailey 1999), and the temperature even in the forenoon period would be more than 1100 K in high solar activity period. In that case, loss due to recombination would increase in high solar activity levels and the NmF2 is less likely to show amplification in the forenoon hours. Therefore, the manifestation of the amplification effect in the forenoon NmF2 may also be a consequence of moderately high level of solar activity (monthly average $F_{10.7} \sim 150$ sfu) during the maximum of solar cycle 24. In the noon and postnoon periods, the transport of ionization from equator due to fountain effect would become very significant over low-latitude region. The development of the EIA and the subsequent extension of the EIA crest to higher latitudes would probably influence the midday and afternoon electron density over Dibrugarh and Okinawa. The daily fountain effect may be related to the midday saturation effect in March equinox as higher density in March equinox could help in NmF2 being saturated with solar activity (Liu et al. 2003). Chen and Liu (2010) also observed the strongest saturation effect in the afternoon of equinox in anomaly crest region and suggested a relationship with equatorial vertical E × B drift. The daytime EIA in solstice is weak, and the crests are closer to the equator (Bhuyan et al. 2003) which may explain the lack of saturation effect in June and December solstices over Dibrugarh. Liu et al. (2006) have shown that neutral composition change and the dynamical effect through the solar activity dependence of hmF2 can also contribute to the NmF2 saturation effect. Therefore, the seasonal difference in midday saturation trend observed in this study may be due to the seasonal variation of neutral composition, thermospheric circulation, temperature, and equatorial electrodynamics. In the postsunset period, production due to photoionization ceases and the F2 layer decays slowly due to chemical recombination. In the low-latitude region, ionization may be transported from equator due to PRE when the zonal electric field is greatly enhanced before reversing its direction from eastward in the daytime to westward in the nighttime. The diurnal variation of seasonally averaged NmF2 in high solar activity period of March equinox and December solstice (Fig. 2) exhibits a plateau or minor peak in the postsunset period around 1900–2000 LT, while in low solar activity period, the evening NmF2 decreases gradually. The evening enhancement in NmF2 (Rao 1963b) is probably related to the strength of PRE which increases with solar activity (Fejer et al. 1979; Scherliess and Fejer 1999). The enhanced electric field also results in enhanced E × B vertical drift and increased altitude of the F2 layer in postsunset period. The amplification effect in December solstice is observed earlier (~1900 LT) as compared to the March equinox (2000 LT) and coincides with the short duration rise of the F2 layer (Fig. 8). This hints at possible role of height rise due to the

PRE in the amplification effect. Therefore, the solar activity variation of postsunset fountain effect and evening height rise via reduced recombination at higher altitudes (Chen et al. 2008) may contribute to increase the postsunset NmF2 non-linearly. The difference in the trends of NmF2 solar activity variation between Dibrugarh and Okinawa may be caused by the longitudinal variation of neutral composition (Oberheide and Forbes 2008; He et al. 2010), temperature (Shepherd et al. 2012), and E × B drifts (Kil et al. 2007). The study of solar activity variation of NmF2 and the winter anomaly ("Diurnal and seasonal variations of NmF2" section) have revealed that the forenoon period NmF2 behaves differently from the midday NmF2. In Fig. 11, we have plotted the monthly average of 1000 LT NmF2, the monthly average of daytime maximum NmF2, and the monthly average $F_{10.7}$ cm flux value for the period of the study. The 1000 LT monthly average NmF2 follows $F_{10.7}$ cm flux closely and mirrors the double-peak structure in solar activity whereas the daytime maximum NmF2 does not. Therefore, we suggest that the forenoon NmF2 in low mid-latitude region is a more sensitive indicator of solar activity variation than the daytime maximum NmF2, and this feature may be useful in empirical modeling studies.

The variation of NmF2 with equatorial electrojet strength

We observed that the forenoon NmF2 is better correlated with solar activity than noon time NmF2. Therefore, to examine the effect of the other dominant mechanism at the low latitude, i.e., electrojet, the variation of hourly NmF2 with maximum electrojet strength over Dibrugarh and Okinawa was investigated for the period of August 2010 till December 2012. The correlation of NmF2 measured at Dibrugarh is high from noon to evening period, whereas for Okinawa, the correlation in the postnoon period is not significant. The variation of midday maximum NmF2 with maximum EEJ for Dibrugarh and Okinawa is shown in Fig. 12. The good correlation of NmF2 with EEJ suggests that in the midday period, electrodynamics is a dominant factor in low latitude. Based on this conjecture, we have examined the joint effect of solar activity and electrojet on midday NmF2 over Dibrugarh and Okinawa by forming a new solar-electromagnetic weighted mean index called low-

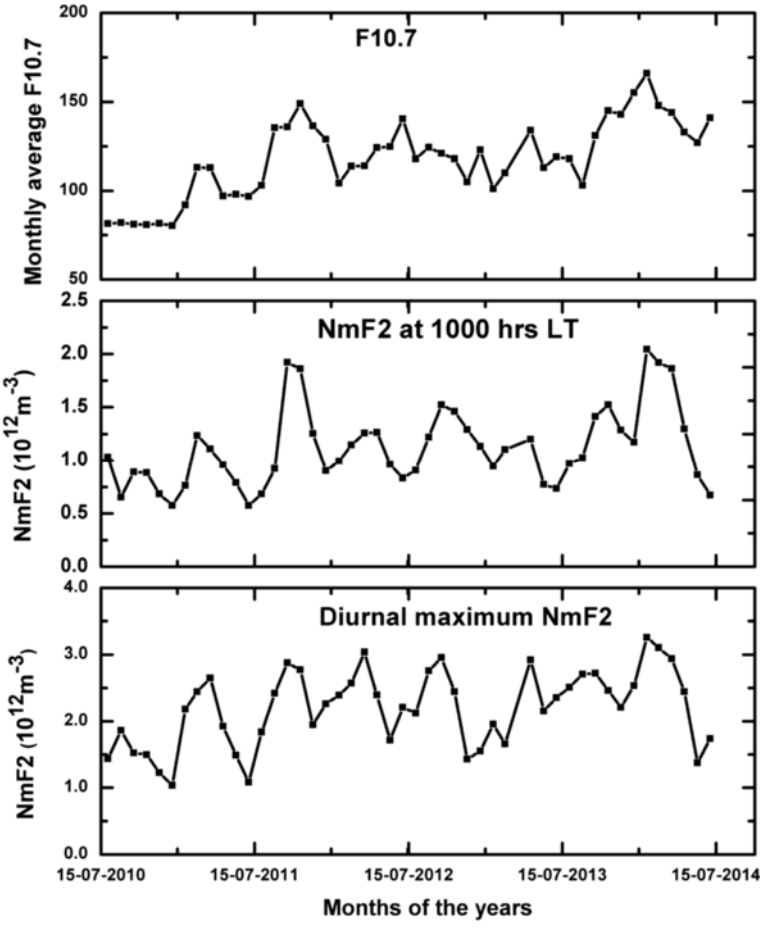

Fig. 11 Double peak in solar proxy F10.7P and monthly mean NmF2 for the period of August 2010–July 2014

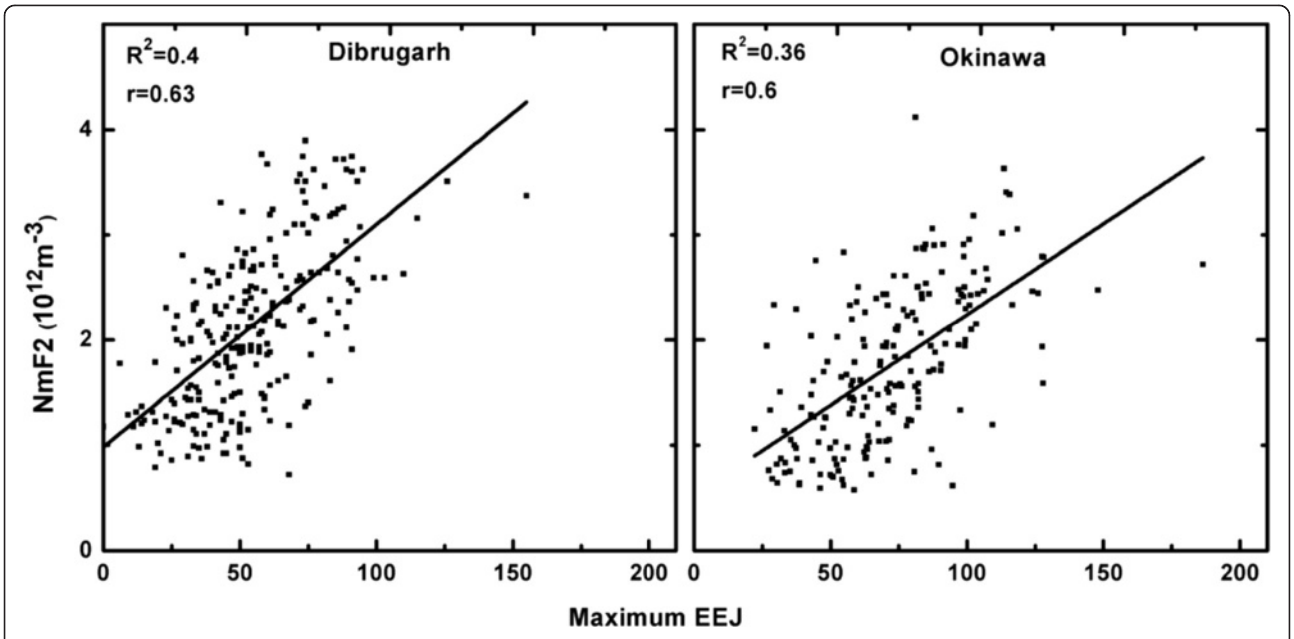

Fig. 12 The scatter plot showing the variation of noon time maximum NmF2 with diurnal maximum EEJ over Dibrugarh and Okinawa

latitude index which is composed of solar activity proxy F107P and maximum electrojet strength., i.e., LowLatIndex = $w_s \times F107P + w_e \times EEJ$ where w_s and w_e are weights for solar activity and electrojet, respectively. Initially, the weights w_s and w_e are assumed as 0.5 and the correlation of the index with daily NmF2 is studied. The weights are changed in small steps till the best correlation is achieved. The final estimated values of w_s and w_e signify the relative contribution of solar flux and EEJ to NmF2 variations. The weights w_s and w_e for Dibrugarh are found to be 0.3 and 0.7, respectively, whereas both the weights for Okinawa are estimated at 0.5. The variation of noon time maximum NmF2 with the LowLatIndex is shown in Fig. 13. The EEJ data period in the figure for Okinawa is August 2010 to April 2014 and for Dibrugarh is August 2010 to December 2012. The midday NmF2 over both the stations shows better correlation with LowLatIndex than with EEJ or solar flux. Therefore, we may suggest that in determining the midday maximum NmF2 over Dibrugarh, the electrojet is relatively more influential than the solar

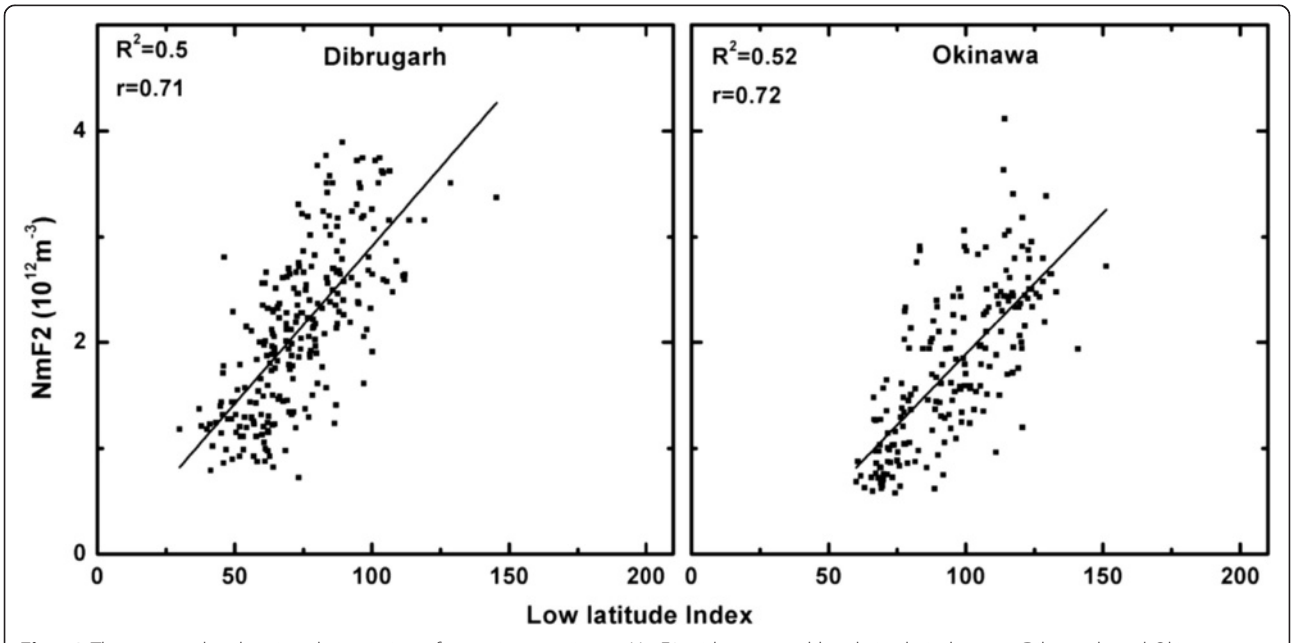

Fig. 13 The scatter plot showing the variation of noontime maximum NmF2 with proposed low latitude index over Dibrugarh and Okinawa

flux but the electrojet and the solar flux are equally important over Okinawa. The daytime WN4 structure in EEJ (England et al. 2006) and the strongest in EEJ peak in 100° E (Lühr et al. 2008) could be the reason for the relatively stronger effect of EEJ over Dibrugarh as compared to that of Okinawa. Further study with a larger data set is required in this direction.

The diurnal and seasonal variations of hmF2 at Dibrugarh and Okinawa

The local time variation and the seasonal average hmF2 for Dibrugarh and Okinawa are presented in Fig. 14. From the figure, it is observed that in low solar activity, the hmF2 over the two stations are almost similar in December solstice. In June solstice and September equinox, hmF2 at Dibrugarh is slightly higher than that of Okinawa during the first half and lower in the second half of the day. In March equinox, nighttime hmF2 over Okinawa is higher than that of Dibrugarh only in the pre-midnight period. Postsunset height rise is observed clearly in December solstice months around 1900 LT. In high solar activity period, the daytime hmF2 over Dibrugarh is significantly higher than that of Okinawa in all seasons, whereas nighttime hmF2 over Dibrugarh is lower than that of Okinawa in June solstice and September equinox. The trends of the ΔhmF2 ($hmF2_{dib} - hmF2_{oki}$) are similar to that of ΔNmF2 in some respect but ΔhmF2 peaks earlier local time as compared to ΔNmF2. The general trend is of higher values over Dibrugarh in the first half of the daytime and lower values in the second half that could be due to the eastward movement of the WN4 structure in the altitude of the F2 layer (Lin et al. 2007b). The higher daytime hmF2 compared to that in the nighttime in all seasons except December solstice and the local time variation of ΔhmF2 suggest that the hmF2 variations may be influenced by the vertical electromagnetic drift which is upward by day and downward by night (Rishbeth et al. 2000). The hmF2 is also affected by neutral winds, diffusion and recombination. In low latitudes, vertical E × B drifts is significant whereas in mid-latitudes, meridional winds become more dominant in controlling the hmF2 [Stubbe and Chandra 1970; Bramley and Ruster 1971; Rishbeth 1971]. It is observed that from around 1900–2000 LT till midnight, the hmF2 tends to increase due to the equator ward meridional winds at night, which pushes the ionization up along the magnetic field lines. Winds could be a dominant factor in Dibrugarh (magnetic dip ~43°, declination ~−0.49°) and Okinawa (magnetic dip ~42°, declination ~−5°) because at 45° magnetic dip, winds produce the maximum effect in height (Titheridge 1995). The hmF2 falls after midnight due to the combined effect of meridional wind, electromagnetic drift, and ambipolar diffusion (Gong et al. 2012). Significant seasonal variation of the diurnal variation of hmF2 is observed in both the stations. From Fig. 14, it is seen that the hmF2 in June solstice and March equinox are higher than those in September equinox and December solstice. The diurnal maximum hmF2 is observed before noon in June solstice and around noon in equinox. These results are also consistent with the earlier observations (Mayr and Mahajan 1971; Sethi et al. 2004). The probable cause of the June–December solstice asymmetry may be the summer to winter interhemispheric neutral winds which would move the ionization along and up the magnetic field lines towards the equator in June solstice and down the field lines towards the pole in December solstice. The high values of hmF2 during March equinox may be caused by higher vertical E × B drift in March equinox (Hazarika and Bhuyan 2014) as well as higher thermospheric temperature (Rishbeth 2004). On the average, a June solstice to December solstice difference of 90 km is observed in daytime hmF2 but the difference is less perceptible in the nighttime. In December solstice, the midnight values of hmF2 are higher than those of daytime maximum hmF2 and this behavior is reminiscent of mid-latitude stations (Mikhailov and Marin 2001; Liu et al. 2007b; Ratovsky and Oinats 2009). It has been reported by number of workers that in the Indian zone, the crest of the EIA recedes in December solstice to ~10° N geomagnetic (Rastogi et al. 1972; Bhuyan et al. 2003; Chakrabarty and Hajra 2009). From the analysis, we may suggest that during December solstice, Dibrugarh/Okinawa behave like mid-latitude stations, whereas in other seasons, they behave more like low-latitude stations. It appears that the hmF2 variations reflect the dynamics of the F2 layer over Dibrugarh and Okinawa as a complex interplay between the vertical E × B drift, temperature, and the meridional neutral winds.

The variation of hmF2 with solar activity and electrojet

The variation of quiet day's hmF2 with the solar activity for the period of September 2010 till April 2014 was examined. Variation of midday hmF2 over Dibrugarh and Okinawa with solar EUV flux and F10.7P is shown in Fig. 15. The correlation of daytime hmF2 over Okinawa with solar activity is relatively poor as compared to that of Dibrugarh. The correlation is highly dependent on season, and the highest and lowest correlations are observed in March equinox and June solstice, respectively. The higher thermospheric turbulence and transequatorial winds may have affected the solar activity correlation during June solstice.

The effect of electrojet on hmF2 over Dibrugarh and Okinawa was compared, and the result is presented in Fig. 16. The correlation of hmF2 over Dibrugarh with electrojet strength varied over the day, and the best correlation ($r \sim 0.57$) was observed for 1400 LT. In the case of Okinawa, correlation of hmF2 with daytime EEJ is not

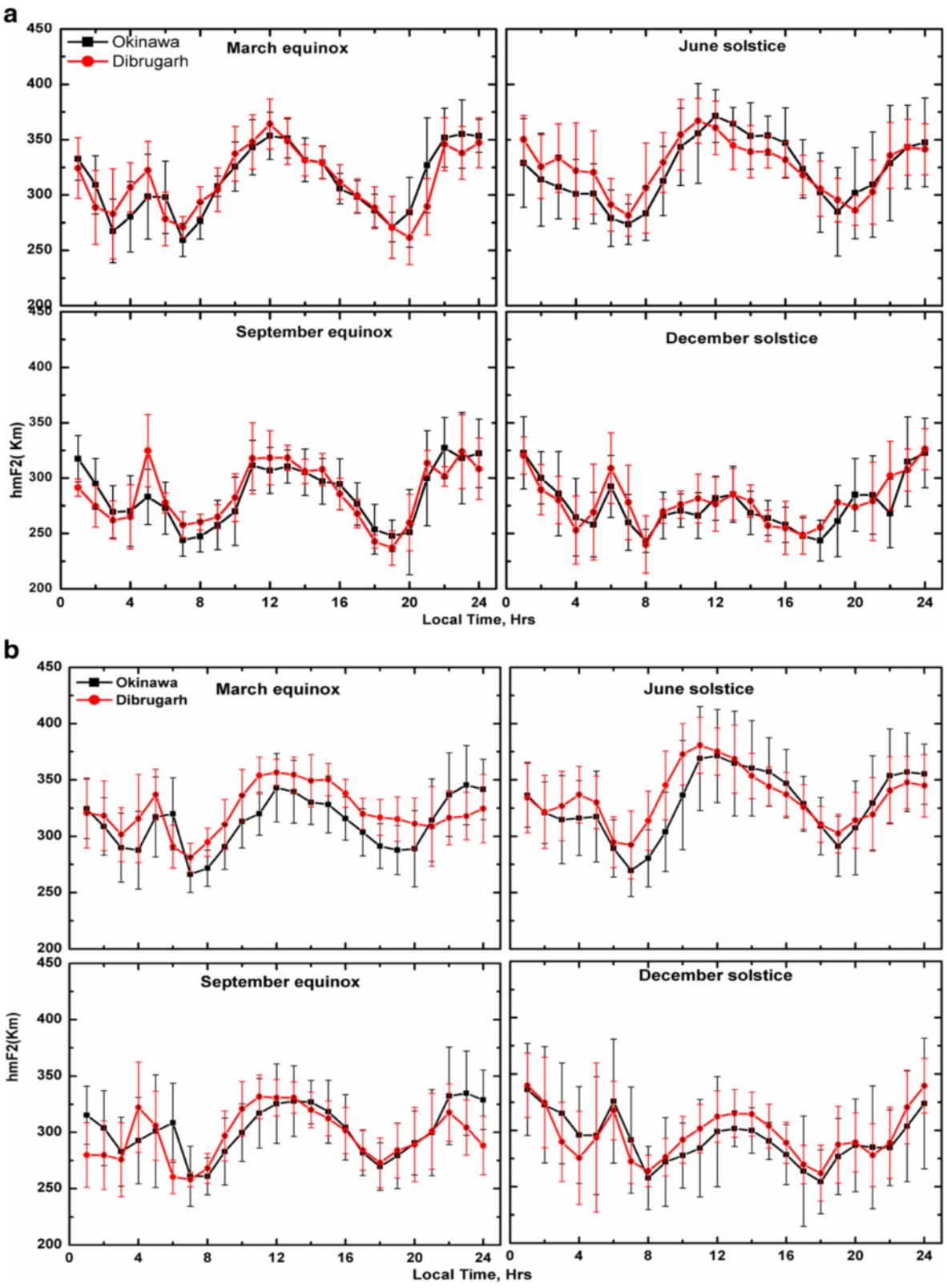

Fig. 14 The seasonal variation of diurnal hmF2 over Dibrugarh and Okinawa for **a** low (September 2010–Aug 2011) and **b** high solar activity (September 2011–April 2014). The *error bars* indicate the standard deviation of the data

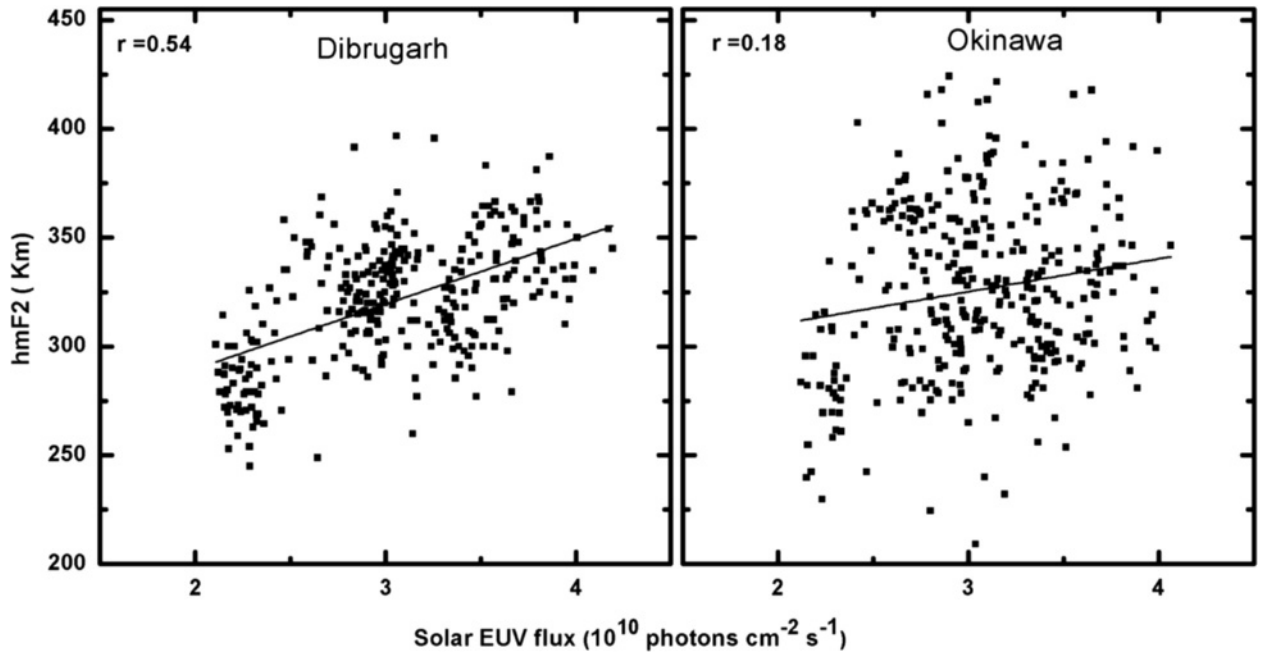

Fig. 15 The scatter plot showing the variation of the midday hmF2 with solar activity

significant. The longitudinal difference in E × B vertical drift (Kil et al. 2007), temperature (Shepherd et al. 2012), and winds may be related to the difference in hmF2 correlations between Dibrugarh and Okinawa. The variation of hmF2 with NmF2 low-latitude index was investigated, but no significant improvement in correlation was observed.

Conclusion

NmF2 and hmF2 measured with a CADI over Dibrugarh at the northern edge of the EIA and within the daytime highest peak of the WN4 structure are studied and compared with that of Okinawa where the nighttime WN4 peak is observed. The simultaneous measurements from Dibrugarh and Okinawa are used to study the local time

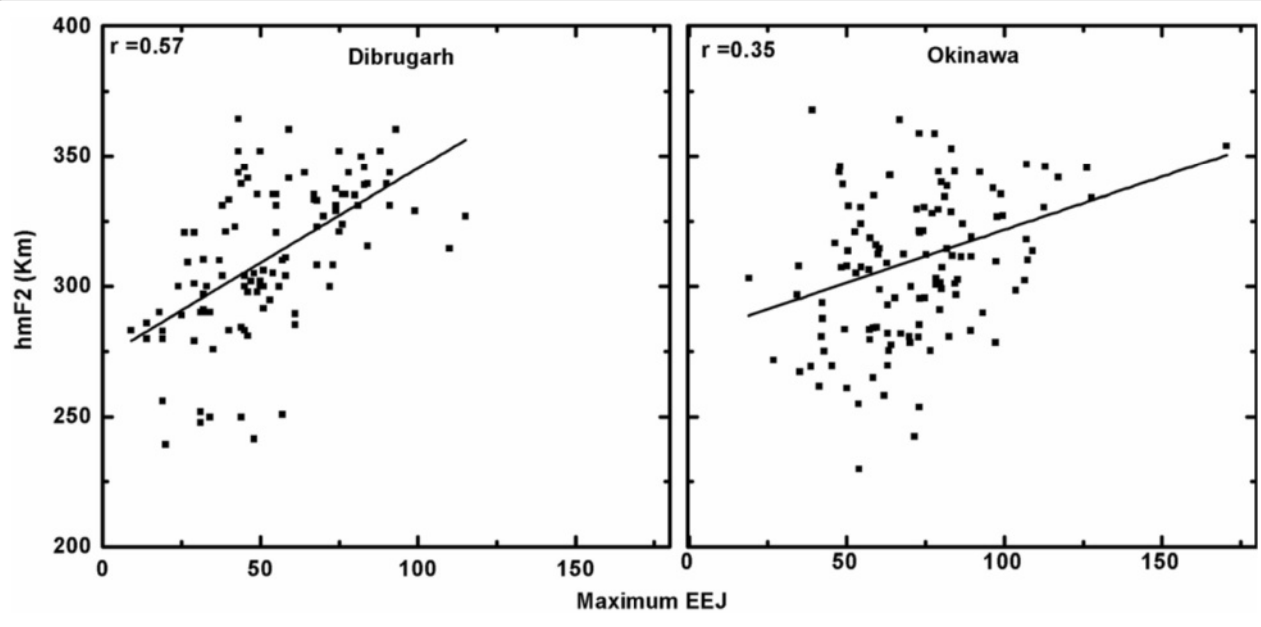

Fig. 16 The scatter plot showing the variation of the midday hmF2 with EEJ

evolution and eastward propagation of the WN4 structure between 95° E and 127° E. The diurnal and seasonal variations of the correlation of NmF2 are suggestive of the physical mechanisms controlling the F2 layer in the low mid-latitude region which change with local time and from season to season. In the morning to forenoon period, the solar flux and neutral composition/thermospheric dynamics is more important than EEJ. Equatorial anomaly and the WN4 structure start to develop in the forenoon, and from then on, the contribution of electrodynamical process also becomes significant. The F2 layer characteristics over the two stations which are in the same geomagnetic latitude but different longitude respond differently to the solar flux and EEJ variations. The longitudinal WN4 structures play a crucial role in shaping the F2 layer characteristics in these stations.

The results are summarized below:

- The winter anomaly in NmF2 over Dibrugarh is absent in low solar activity levels and is manifested in moderate to high solar activity levels only.
- The eastward propagation speed of the WN4 structure estimated from local time difference of NmF2 is found to be about 4.3°/h in low solar activity period and about 3.2°/h in high solar activity period.
- The correlation of NmF2 with solar EUV flux/F10.7P exhibits diurnal variation with maximum in the forenoon hours. The degree of correlation of NmF2 with solar activity and its diurnal variation exhibit seasonal dependence. Correlation is highest in equinox, especially in March equinox. The forenoon NmF2 is more sensitive to solar flux variations than the midday NmF2 in low mid-latitude region.
- The NmF2 in March equinox exhibits a tendency for amplification with solar activity in the forenoon and postsunset periods. The NmF2 in the midday period of equinox is more likely to saturate with solar activity. Amplification is also observed in the postsunset period of December solstice. The forenoon amplification effect may be a manifestation of unique location of the two stations and the moderate level of solar activity in the maximum of solar cycle 24. Further study involving a larger data set will probably validate these results.
- The influence of EEJ in determining the midday NmF2 is relatively stronger over Dibrugarh than over Okinawa, and the result may be attributed to the longitudinal wave structure in EEJ.
- A new composite weighted mean index of F10.7P and EEJ is proposed for low-latitude region. The midday maximum NmF2 is shown to exhibit better correlation with this new index.

Competing interests
The authors declare that they have no competing interests.

Authors' contributions
B.R. Kalita was involved in collecting the ionospheric data for Dibrugarh. He also analyzed all the data and planned and prepared the manuscript. Prof. P.K. Bhuyan is heading the project under which the Dibrugarh ionosonde is operating and was actively involved in the analyzing the results and preparing the manuscript. Dr. Akimasa Yoshikawa provided the magnetic data in the 120° E longitude under the MAGDAS project and actively participated in preparing the manuscript. All authors read and approved the final manuscript.

Acknowledgements
The CADI ionosonde in Dibrugarh was installed and operated as part of Indian Space Research Organization's Space Science Promotion Scheme. The authors would like to thank IIG, Mumbai for the magnetic observatory data in the Indian zone. The MAGDAS/CPMN magnetic data of DAV and MUT were provided by the PI of MAGDAS/CPMN project (http://magdas.serc.kyushu-u.ac.jp/). This work was supported in part by JSPS Core-to-Core Program, B. Asia-Africa Science Platforms. The authors would like to thank Teiji Uozumi for the processing of the MAGDAS/CPMN magnetic data. The $F_{10.7}$ cm flux data and magnetic data (K_p) can be downloaded freely from http://spidr.ngdc.noaa.gov/spidr/. The daily values of the SEM/SOHO EUV fluxes can be obtained from http://www.usc.edu/dept/space_science/semdatafolder/long/.

Author details
[1]Center for Atmospheric Studies, Dibrugarh University, Dibrugarh 786004, Assam, India. [2]Department of Earth and Planetary Sciences, International center for Space Weather Science and education (CSWSE:イクセイ=育成), Kyushu University, Fukuoka, Japan.

Received: 14 May 2015 Accepted: 5 November 2015
Published online: 19 November 2015

References
Adebesin BO, Adeniyi JO, Adimula IA, Reinisch BW, Yumoto K (2013) F2 layer characteristics and electrojet strength over an equatorial station. Adv Space Res 52(5):791–800
Alken P et al (2013) Swarm SCARF equatorial electric field inversion chain. Earth, Planets and Space 65(11):1309–1317
Appleton EV (1946) Two anomalies in the ionosphere. Nature 157:691
Bailey DK (1948) The geomagnetic nature of the F2-layer longitude-effect. Terr Mag Atmo Elec 53(1):35–39. doi:10.1029/TE053i001p00035
Balan N, Bailey GJ, Jayachandran B (1993) Ionospheric evidence for a nonlinear relationship between the solar e.u.v. and 10.7 cm fluxes during an intense solar cycle. Planet Space Sci 41:141–145. doi:10.1016/0032-0633(93)90043-2
Balan N, Bailey GJ, Jenkins B, Rao PB, Moffet J (1994) Variations of ionospheric ionization and related solar fluxes during an intense solar cycle. J Geophys Res 99:2243–2253. doi:10.1029/93JA02099
Balan N, Otsuka Y (1998) Equinoctial asymmetries in the ionosphere and thermosphere observed by the MU radar. J Geophys Res: 103(A5):9481–9495
Bhuyan PK, Tyagi TR, Singh L, Somayajulu YV (1983) Ionospheric electron content measurements at northern low midlatitude station through half solar cycle. Ind JRad Spac Phy 12:84–93
Bhuyan PK, Chamua M, Bhuyan K, Subrahmanyam P, Garg SC (2003) Diurnal, seasonal and latitudinal variation of electron density in the topside F-region of the Indian zone ionosphere at solar minimum and comparison with IRI. J Atmos Sol-Terr Phys 65:359–368
Bhuyan PK, Hazarika R (2012) GPS TEC near the crest of the EIA at 95°E during the ascending half of solar cycle 24 and comparison with IRI simulations. Adv Space Res 52:1247–1260
Booker HG, Smith EK (1970) A comparative study of ionospheric measurement techniques. J Atmos Terr Phys: 32(4):467–497
Bramley EN, Ruster R (1971) The effect of electric fields and ion drag in the middle latitude F-region. J Atmos Terr Phy 33(2):269–274
Buonsanto MJ (1999) Ionospheric storms: a review. Space Science Review 88:563–601
Cardoso FA, Sahai Y, Guarnieri FL, Fagundes PR, Pillat VG, da Silva JVPR (2011) Dependence of the F-region peak electron density (NmF2) on solar activity

observed in the equatorial ionospheric anomaly region in the Brazilian sector. Adv Space Res 48:837–841
Chakrabarty SK, Hajra R (2009) Electrojet control of ambient ionization near the crest of the equatorial anomaly in the Indian zone. Ann Geophy: 27:93–105
Chandra H, Rastogi RG (1974) Geomagnetic storm effects on ionospheric drifts and the equatorial Es over the magnetic equator. Ind J Radio Space Phys 3: 332–336
Chen Y, Liu L, Le H (2008) Solar activity variations of nighttime ionospheric peak electron density. J Geophys Res 113, A11306. doi:10.1029/2008JA013114
Chen Y, Liu L, Wan W, Yue X, Su S-Y (2009) Solar activity dependence of the topside ionosphere at low latitudes. J Geophys Res 114, A08306. doi:10.1029/2008JA013957
Chen Y, Liu L (2010) Further study on the solar activity variation of daytime NmF2. J Geophys Res: 115, A12337. doi:10.1029/2010JA015847
Chen Y, Liu L, Wan W (2011) Does the $F_{10.7}$ index correctly describe solar EUV flux during the deep solar minimum of 2007–2009? J Geophys Res 116:A4. doi:10.1029/2010JA016301
Chen Y, Liu L, Wan W, Ren Z (2012) Equinoctial asymmetry in solar activity variations of NmF2 and TEC. Ann Geophys 30:613–622, http://dx.doi.org/10.5194/angeo-30-613-2012
Dabas RS, Bhuyan PK, Tyagi TR, Bhardwaj RK (1984) Day-to-day changes in ionospheric electron content at low latitudes. Radio Science 19(3):749–756
Dabas RS, Sharma N, Pillai MGK, Gwal AK (2006) Day-to-day variability of equatorial and low latitude F-region ionosphere in the Indian zone. J Atmos and Sol-Terr Phys: 68(11):1269–1277
Danilov AD, Lastovicka J (2001) Effects of geomagnetic storms on the ionosphere and atmosphere. International Journal of Geomagnetism and Aeronomy 2:3
Da Rosa AV, Waldman H, Bendito J, Garriott OK (1973) Response of the ionospheric electron content to fluctuations in solar activity. J Atmos Terr Phys 35:1429
Deminova GF (1993) Wave structure of longitudinal variations in the nighttime equatorial ionosphere. Geomagn Aeron 33(5):167–169
Deminova GF (1995) Wave structure of longitudinal variations in the nighttime equatorial anomaly. Geomag Aeron 35(4):169–173
Deshpande MR, Rastogi RG, Vats HO, Kulbtchar J, Sethi G (1977) Effect of electrojet on the total electron content of the ionosphere over the Indian subcontinent. Nature 267:599–600, doi:10.1038/267599a0.
Essex EA (1977) Equinoctial variations in the total electron content of the ionosphere at northern and southern hemisphere stations. J Atmos Terr Phys 39:645
England SL, Maus S, Immel TJ, Mende SB (2006) Longitudinal variation of the E-region electric fields caused by atmospheric tides. Geophys Res Lett 33, L21105. doi:10.1029/2006GL027465
Fang TW, Kil H, Millward G, Richmond AD, Liu JY, Oh SJ (2009) Causal link of wave-4 structure in plasma density and vertical plasma drift in low latitude ionosphere. J Geophys Res 114:A10315. doi:10.1029/2009JA014460
Fejer BG, Farley DT, Woodman RF, Calderon C (1979) Dependence of equatorial F-region vertical drifts on season and solar cycle. J Geophys Res 84:5792
Fejer BG, Jensen JW, Su S-Y (2008) Quiet time equatorial F region vertical plasma drift model derived from ROCSAT-1 observations. J Geophys Res 113, A05304. doi:10.1029/2007JA012801
Field P, Rishbeth RH (1997) The response of the ionospheric F2-layer to geomagnetic activity (1997) an analysis of worldwide data. J Atmos Terr PhysPhysics 59(2):163–180, http://dx.doi.org/10.1016/S1364-6826(96)00085-5
Gong Y, Zhou Q, Zhang S, Aponte N, Sulzer M, Gonzalez S (2012) Midnight ionosphere collapse at Arecibo and its relationship to the neutral wind, electric field, and ambipolar diffusion. J Geophys Res 117, A08332. doi:10.1029/2012JA017530
Hazarika R, Bhuyan PK (2014) Spatial distribution of TEC across India in 2005: seasonal asymmetries and IRI predictions. Adv Space Res 54(9):1751–1767. doi:10.1016/j.asr.2014.07.011
He M, Liu L, Wan W, Lei J, Zhao B (2010) Longitudinal modulation of the O/N_2 column density retrieved from TIMED/GUVI measurement. Geophys Res Lett 37, L20108. doi:10.1029/2010GL045105
Henderson SB, Swenson CM, Christensen AB, Paxton LJ (2005) Morphology of the equatorial anomaly and equatorial plasma bubbles using image subspace analysis of global ultraviolet imager data. J Geophys Res 110:A11306, http://dx.doi.org/10.1029/2005JA011080
Hierl PM, Dotan I, Seeley JV, Van Doren JM, Morris RA, Vigiano AA (1997) Rate constants for the reactions of O + with N2 and O2 as a function of temperature (300-1800 K). J Chem Phys 106:3540–3544
Ikubanni SO, Adeniyi JO (2013) Variation of saturation effect in the ionospheric F2 critical frequency at low latitude. J Atmos Terr Phys 100–101, 24–33, ISSN 1364-6826. http://dx.doi.org/10.1016/j.jastp.2013.03.012.
Immel TJ, Sagawa E, England SL, Henderson SB, Hagan ME, Mende SB, Frey HU, Swenson CM, Paxton LJ (2006) The control of equatorial ionospheric morphology by atmospheric tides. Geophys Res Lett 33, L15108. doi:10.1029/2006GL026161
Jin H, Miyoshi Y, Fujiwara H, Shinagawa H (2008) Electrodynamics of the formation of ionospheric wave number 4 longitudinal structure. JGeophysRes 113:A09307
Kane RP (1992) Sunspots, solar radio noise, solar EUV and ionospheric NmF2. J Atmos Terr Phys 54:463–466
Kane RP (2006) Are the double-peaks in solar indices during solar maxima of cycle 23 reflected in ionospheric NmF2? J Atmos Sol-Terr Phys 68(8):877–880
Kil H, Oh S-J, Kelley MC, Paxton LJ, England SL, Talaat E, Min K-W, Su S-Y (2007) Longitudinal structure of the vertical E × B drift and ion density seen from ROCSAT-1. Geophysical Res Lett 34. doi:10.1029/2007GL030018. issn: 0094-8276.
Kil H, Talaat ER, Oh SJ, Paxton LJ, England SL, Su SY (2008) Wave structures of the plasma density and vertical E × B drift in low-latitude F region. J Geophys Res 113:A09312, http://dx.doi.org/10.1029/2008JA013106
Lin CH, Wang HME, Hsiao CC, Immel TJ, Hsu ML, Liu JY, Paxton LJ, Fang TW, Liu CH (2007a) Plausible effect of atmospheric tides on the equatorial ionosphere observed by the FORMOSAT-3/COSMIC: three-dimensional electron density structures. Geophys Res Lett 34, L11112. doi:10.1029/2007GL029265
Lin CH, Hsiao CC, Liu JY, Liu CH (2007b) Longitudinal structure of the equatorial ionosphere: the evolution of the four peaked structure. J Geophys Res 112, A12305. doi:10.1029/2007JA012455
Liu JY, Chen YI, Lin JS (2003) Statistical investigation of the saturation effect in the ionospheric NmF2 versus sunspot, solar radio noise and solar EUV radiation. J Geophys Res 108(A2):1067, http://dx.doi.org/10.1029/2001JA007543
Liu L, Wan W, Ning B (2004) Statistical modelling of ionospheric NmF2 over Wuhan. Radio Sci 39:RS2013. doi:10.1029/2003RS003005
Liu L, Wan W, Ning B, Piog OM, Kurkin VI (2006) Solar activity variations of the ionospheric peak electron density. J Geophys Res 111:A08304, http://dx.doi.org/10.1029/2006JA011598
Liu L, Wan W, Yue X, Ning B, Zhang ML (2007a) The dependence of plasma density in the topside ionosphere on the solar activity level. Ann Geophys 25:1337–1343
Liu L, Wan W, Zhang ML, Ning B, Zhang SR (2007b) Variations of topside ionospheric scale heights over Millstone Hill during the 30-day incoherent scatter radar experiment. Ann Geophys: 25(9):2019–2027
Liu H, Watanabe S (2008) Seasonal variation of the longitudinal structure of the equatorial ionosphere: does it reflect tidal influences from below? J Geophys Res 113, A08315. doi:10.1029/2008JA013027
Liu J, Liu L, Zhao B, Lei J, Wan W (2011) On the relationship between the postmidnight thermospheric equatorial mass anomaly and equatorial ionization anomaly under geomagnetic quiet conditions. J Geophys Res 116, A12312. doi:10.1029/2011JA016958
Liu J, Liu LB, Zhao BQ, Wan WX, Chen YD (2012) Empirical modeling of ionospheric F2 layer critical frequency over Wakkanai under geomagnetic quiet and disturbed conditions. Science China Technological Sciences 55(5):1169–1177
Lühr H, Hausler K, Stolle C (2007) Longitudinal variation of F region electron density and thermospheric zonal wind caused by atmospheric tides. Geophys Res Lett 34, L16102. doi:10.1029/2007GL030639
Lühr H, Rother M, Hausler K, Alken P, Maus S (2008) Influence of nonmigrating tides on the longitudinal variation of the equatorial electrojet. J Geophys Res 113, A08313. doi:10.1029/2008JA013064
Mayr HG, Mahajan KK (1971) Seasonal variation in the F_2 region. J Geophys Res 76(4):1017–1027
Ma R, Xu J, Wang W, Yuan W (2009) Seasonal and latitudinal differences of the saturation effect between ionospheric NmF2 and solar activity indices. J Geophys Res 114, A10303. doi:10.1029/2009JA014353
Mikhailov AV, Marin D (2001) An interpretation of the *NmF2* and *hm*F2 long-term trends in the framework of the geomagnetic control concept. Ann Geophy 19:733–748
Mikhailov AV, Perrone L (2011) On the mechanism of seasonal and solar cycle NmF2 variations: a quantitative estimate of the main parameters contribution using incoherent scatter radar observations. J Geophys Res 116, A03319. doi:10.1029/2010JA016122
Oberheide J, Forbes JM (2008) Thermospheric nitric oxide variability induced by nonmigrating tides. Geophys Res Lett 35, L16814. doi:10.1029/2008GL034825

Oh S, Kil H, Kim WT, Paxton LJ, Kim YH (2008) The role of the vertical E × B drift for the formation of the longitudinal plasma density structure in the low-latitude F region. Ann Geophys 26:2061–2067
Rao BNC (1963a) Some characteristic features of the equatorial ionosphere and the location of the *F*-region equator, 1963. J Geophys Res 68(9):2541–2549
Rao BNC (1963b) The postsunset rise of f_oF_2 in the transition region and its dependence on the postsunset rise of *h'F* in the equatorial region, 1963. J Geophys Res 68(9, 1): 2551–2557
Rastogi RG, Sanatani S (1968) Forenoon bite-out of F2 layer ionization at tropical latitudes. Ann Geophys 24:75–80
Rastogi RG, Chandra H, Sharma RP, Rajaram G (1972) Ground based measurements of ionospheric phenomenon associated with the equatorial electrojet. IndJRadioSpace Phys 1:119–135
Ratovsky KG, Oinats AV (2009) Medvedev AV Diurnal and seasonal variations of F2 layer characteristics over Irkutsk during the decrease in solar activity in 2003–2006: observations and IRI-2001 model predictions. Advances in Space Research 43:1806–1811
Ren Z, Wan W, Liu L, Xiong J (2009) Intra-annual variation of wave number 4 structure of vertical E × B drifts in the equatorial ionosphere seen from ROCSAT-1. J Geophys Res 114, A05308. doi:10.1029/2009JA014060
Ren Z, Wan W, Xiong J, Liu L (2014) Influence of DE3 tide on the equinoctial asymmetry of the zonal mean ionospheric electron density. Earth, Planets and Space 66:117. doi:10.1186/1880-5981-66-117
Rishbeth H (1971) Thermospheric winds and the *F*-region: a review. J Atmos Terr Phy 34:1–47
Rishbeth H, Garriott OK (1969) Introduction to Ionospheric Physics, Elsevier, New York.
Rishbeth H, Sedgemore-Schulthess KJF, Ulich (2000) The semiannual and annual variations in the height of the ionospheric F2-peak. Ann Geophy 18:285–299
Rishbeth H (2004) Questions of the equatorial F2-layer and thermosphere. J Atmos Sol-Terr Phys 66:1669–1674
Rush CM, Richmond AD (1973) The relationship between the structure of the equatorial anomaly and the strength of the equatorial electrojet. J Atmos Terr Phy 35(6):1171–1180
Sagawa E, Immel TJ, Frey H, Mende SB (2005) Longitudinal structure of the equatorial anomaly in the nighttime ionosphere observed by IMAGE/FUV. J Geophys Res 110:A11302, http://dx.doi.org/10.1029/2004JA010848
Sastri JH (1990) The relationship between the structure of the equatorial anomaly and the strength of the equatorial electrojet. Ind J Radio Space Phys 19:225–240
Scherliess L, Fejer BG (1999) Radar and satellite global equatorial *F* region vertical drift model. J Geophys Res 104(A4):6829–6842. doi:10.1029/1999JA900025
Scherliess L, Thompson DC, Schunk RW (2008) Longitudinal variability of low-latitude total electron content: tidal influences. J Geophys Res 113:A01311, http://dx.doi.org/10.1029/2007JA012480
Sethi NK, Goel MK, Mahajan KK (2002) Solar cycle variations of NmF2 from IGY to 1990. Ann Geophys 20:1677–1685
Sethi NK, Dabas RS, Vohra VK (2004) Diurnal and seasonal variations of *hm*F2 deduced from digital ionosonde over New Delhi and its comparison with IRI 2001. Ann Geophys 22:453–458
Shepherd MG, Shepherd GG, Cho Y-M (2012) Longitudinal variability of thermospheric temperatures from WINDII O(^{1}S) dayglow. J Geophys Res 117, A10302. doi:10.1029/2012JA017777
Simi KG, Manju G, Madhav Haridas MK, Prabhakaran Nayar SR, Tarun Kumar Pant, Alex S (2013) Ionospheric response to a geomagnetic storm during November 8-10, 2004, Earth, Planets and Space, April 2013, 65(4):343–350
Stubbe P, Chandra S (1970) The effect of electric fields on the *F*-region behaviour as compared with neutral wind effects. J Atmos Terr Phy 32(12):1909–1919
Su YZ, Bailey GJ (1999) Altitude dependencies in the oslar activity variations of the ionospheric electron density. J Geophys Res 104:47,14879–14891
Titheridge JE (1973) The electron content of the southern midlatitude ionosphere, 1965-1971. J Atmos Terr Phys 981–1001
Titheridge J (1985) Ionogram analysis with the generalized Program POLAN, World Data Center Rep. UAG-93 World Data Cent. for SolarTerrestrial Physics, Boulder, Colorado, (http://www.sws.bom.gov.au/IPSHosted/INAG/uag_93/uag_93.html)
Titheridge J (1995) Winds in the ionosphere—a review. J Atmos Terr Phys 57(14):1681–1714
Thomas L (1968) The F2-region equatorial anomaly during solstice periods at sunspot maximum. J Atmos Terr Phys 30:1631–1640
Walker GO, Ma JHK (1972) Influence of solar flux and the equatorial electrojet on the diurnal development of the latitude distribution of total electron content in the 'equatorial anomaly'. J Atmos Terr Phys 34(8):1419–1424
Walker GO (1981) Longitudinal structure of the F-region equatorial anomaly—a review. J Atmos Terr Phys 43:763
Watthanasangmechai K, Yamamoto M, Saito A, Maruyama T, Yokoyama T, Nishioka M, Ishii M (2015) Temporal change of EIA asymmetry revealed by a beacon receiver network in Southeast Asia. Earth, Planets and Space 67:75. doi:10.1186/s40623-015-0252-9
Wichaipanich N, Supnithi P, Tsugawa T, Maruyama T (2012) Thailand low and equatorial F2-layer peak electron density and comparison with IRI-2007 model. Earth, Planets and Space 64(6):485–491
Yadav S, Dabas RS, Das RM, Upadhayaya AK, Sharma K (2010) Gwal A (2009) Diurnal and seasonal variation of F2-layer ionospheric parameters at equatorial ionization anomaly crest region and their comparison with IRI-2001. Adv Spac Res 45:361–367
Yadav S, Dabas RS, Das RM, Upadhayaya AK, Sarkar SK, Gwal AK (2011) Variation of F-region critical frequency (NmF2) over equatorial and low-latitude region of the Indian zone during 19th and 20th solar cycle. Adv Spac Res 47(1):124–137